A STUDY OF CSCL TYPE INTERMEDIATE PHASES INVOLVING RARE EARTH ELEMENTS

Thesis by

Chang-Chih Chao

In Partial Fulfillment of the Requirements -

For the Degree of

Doctor of Philosophy

California Institute of Technology

Pasadena, California

1965

(Submitted May 24, 1965)

ACKNOWLEDGEMENT

The author wishes to express his deepest thanks to Professor Pol Duwez for his encouragement and help throughout this work and his great patience on reading and correcting the manuscript. It is with deep appreciation also that I thank Professor F. S. Buffington for his reading the manuscript and helpful suggestions, and to Professors R. Mössbauer and M. S. Plesset for their reading the manuscript.

Thanks are due to Dr. J. W. Cable for communicating his results of neutron diffraction analysis of some of the CsCl phases supplied by the author and to Professor Mössbauer for communicating the magnetic susceptibility measurements of Dr. R. Walline of the University of Pittsburgh.

Finally, it is a pleasure to acknowledge the research grant from the Atomic Energy Commission which has made this study possible.

ABSTRACT

This thesis presents the results of a systematic study of CsCl type phases in binary alloys of rare earth elements with other metals. Thirty-nine new phases of this type have been found. The linear variation of the lattice parameter of CsCl phases with the trivalent ionic radius of the rare earth metal previously established for a limited number of alloys, has been extended to seventy-nine phases. This linear relationship leads to some interesting qualitative arguments on the ionic size of the non-rare earth element in these phases. The electrical resistivities of nineteen CsCl type phases of rare earths with copper, silver and gold were measured between 4.2°K and about 250°K. With the exception of the yttrium-silver phase, all others exhibited an anomaly in the resistivity-temperature curve which is attributed to an antiferromagnetic transition. This conclusion is confirmed by previously published results of neutron diffraction experiments and magnetic susceptibility measurements. A qualitative interpretation of the resistivity results based on the indirect exchange interaction between the ions of the same type (magnetic or non-magnetic) and between the ions of the different type (magnetic and non-magnetic) is proposed.

CONTENTS

I. INTRODUCTION 1

II. ALLOYS INVESTIGATED AND EXPERIMENTAL TECHNIQUE 4

III. NEW CSCL PHASES 11

A. LATTICE PARAMETER-MEASUREMENTS

B. CORELATION BETWEEN LATTICE PARAMETERS AND TRIVALENT IONIC RADII

IV. ELECTRICAL RESISTIVITY OF CSCL PHASES 24

A. SPECIMEN PREPARATION AND EXPERIMENTAL METHODS

B. RESULTS

C. DISCUSSION

V. THEORETICAL CONSIDERATION ON THE RESISTIVITY-TEMPERATURE RELATIONSHIP IN CSCL PHASES CONTAINING RARE EARTH ELEMENTS 62

VI. ANALYSIS OF THE ANTIFERROMAGNETIC TRANSITION IN CSCL PHASES CONTAINING RARE EARTH ELEMENTS 76

VII. CONCLUSIONS 84

REFERENCES 86

LIST OF TABLES

1. Lattice Parameters of The CsCl Type Phases Involving Rare Earth Elements 2

2. Alloys Studied in This Investigation 5

3. Impurity Analysis of The Elements Used in This Study 6

4. Lattice Parameters of Intermediate Phases with CsCl Type Crystal Structure Involving Rare Earth Elements 12

5. Characteristic Values for CsCl Phases Involving Rare Earth Elements 15

6. Radii (Atomic and Ionic) and Electronegativity of the Metals in CsCl Phases 21

7. Lattice Parameters of CsCl Phases 23

8. CsCl Phases Used For Electrical Resistivity-Temperature Measurements 28

9. Transition Temperature or Temperature Range of CsCl Phases 52

10. Summary of Results on the Resistivity-Temperature Curves of CsCl Phases 61

11. Comparison of the Magnetic Moment of Rare Earth Ions in CsCl Phases and in Pure Elements 77

12. Resistivity of CsCl Phases and of Pure Rare Earth Elements Due To Spin-Disorder Scattering 81

LIST OF FIGURES

1. Relationship between The Trivalent Ionic Radii of Rare Earth Elements and The Lattice Parameters of CsCl Phases 19

2. Resistivity-Temperature Relationship for YAg Intermediate Phase 29

3. Resistivity-Temperature Relationship for NdAg Intermediate Phase 30

4. Resistivity-Temperature Relationship for GdCu Intermediate Phase 32

5. Resistivity-Temperature Relationship for GdAg Intermediate Phase 33

6. Resistivity-Temperature Relationship for GdAu Intermediate Phase 34

7. Resistivity-Temperature Relationship for TbCu Intermediate Phase 35

8. Resistivity-Temperature Relationship for TbAg Intermediate Phase 36

9. Resistivity-Temperature Relationship for TbAu Intermediate Phase 37

10. Resistivity-Temperature Relationship for DyCu Intermediate Phase 38

11. Resistivity-Temperature Relationship for DyAg Intermediate Phase 39

12. Resistivity-Temperature Relationship for DyAu Intermediate Phase 40

13. Resistivity-Temperature Relationship for HoCu Intermediate Phase 41

14. Resistivity-Temperature Relationship for HoAg Intermediate Phase 42

15. Resistivity-Temperature Relationship for HoAu Intermediate Phase 43

16. Resistivity-Temperature Relationship for ErAg Intermediate Phase 44

LIST OF FIGURES (continued)

17. Resistivity-Temperature Relationship for ErAu Intermediate Phase 45

18. Resistivity-Temperature Relationship for TmCu Intermediate Phase 46

19-1. Resistivity-Temperature Relationship for TmAg Intermediate Phase 47

19-2. Resistivity-Temperature Relationship for TmAg Intermediate Phase 48

20-1. Resistivity-Temperature Relationship for TmAu Intermediate Phase 49

20-2. Resistivity-Temperature Relationship for TmAu Intermediate Phase 50

21. Comparison of The Resistivity-Temperature Curves of the RCu Intermediate Phases 53

22. Comparison of The Resistivity-Temperature Curves of the RAg Intermediate Phases 54

23. Comparison of The Resistivity-Temperature Curves of the RAu Intermediate Phases 55

24. Comparison of The Resistivity-Temperature Curves of the CsCl Phases of GdCu, Ag and Au 56

25. Comparison of The Resistivity-Temperature Curves of the CsCl Phases of Tb, Dy and Cu, Ag, Au 57

26. Comparison of The Resistivity-Temperature Curves of the CsCl Phases of Ho, Er and Tm with Cu, Ag, Au 58

27. The Relationship Between The Resistivity due to The Spin-Disorder Scattering and The Value of $(g-1)^2(J-1)J$ of Rare Earth Ions in CsCl Phases 82

I. INTRODUCTION

The metals known as the Rare Earths (from Lanthanum, atomic number 57 to Lutecium, atomic number 71) are rather late comers in the metallurgical literature. Before about 1930, probably because of the complexity of the extractive metallurgical problems involved, most of the rare earth metals were not available with a sufficient degree of purity to justify systematic studies of their alloying behavior. From then on, however, a large number of investigators showed an interest in rare earth metallurgy, and contributed to knowledge of the intermediate phases between rare earth metals and other metallic elements. The first CsCl type intermediate phase was reported in 1933 in praseodymium-magnesium alloys and in the following years, approximately sixty CsCl type intermediate phases were reported. A summary of the CsCl type intermediate phases is presented in TABLE 1, in which the lattice parameter and the references to the original publications are included. From this table, it can be seen that the metals alloyed with a rare earth element includes those of the I B column of the periodic table (Cu, Ag, and Au), the II B column (Zn, Cd, and Hg), the III A column (Al, In, and Tl), in addition to Mg (II A column) and only one transition element, namely Rh. In spite of the rather large number of CsCl phases reported, it is obvious that many additional binary alloys remain to be investigated before a complete systematic analysis can be made on the factors affecting the existence of these phases. One of the purposes of the present study was to discover additional CsCl

TABLE 1

Lattice Parameters of The CsCl Type Phases
Involving Rare Earth Elements

	Mg	Al	Cu	Zn	Ag	Cd	In	Au	Hg	Tl	Rh
Sc					3.43 (1)			3.38 (1)			3.206 (24)
Y	3.80 (9)		3.476 (15)	3.577 (2)	3.617 (17)			3.559 (1)			3.411 (25)
La	3.967 (5, 6)	3.79 (11)		3.759 (16)	3.781 (19)	3.905 (16)			3.845 (22)	3.922 (18)	
Ce	3.899 (6, 7)	3.86 (12)		3.704 (16)	3.746 (19)	3.865 (16)			3.816 (22)	3.893 (18)	
Pr	3.888 (8)			3.678 (16)	3.739 (18)	3.830 (16)		3.68 (1)	3.799 (22)	3.869 (18)	
Nd	3.867 (8)	3.74 (13)		3.667 (2)	3.714 (20)	3.811 (8)		3.659 (1)	3.780 (22)		
Sm	3.810 (8)		3.528 (2)	3.627 (2)	3.673 (1)	3.771 (8)		3.621 (1)	3.744 (8)	3.813 (8)	
Eu											
Gd	3.824 (10)		3.505 (2)	3.602 (2)	3.6476 (21)			3.593 (1)			
Tb	3.796 (10)		3.480 (2)	3.576 (2)	3.625 (1)			3.576 (1)	3.678 (23)		
Dy	3.786 (10)	3.71 (14)	3.460 (2)	3.563 (2)	3.608 (21)			3.555 (1)			
Ho	3.776 (10)		3.445 (2)	3.547 (2)	3.592 (1)			3.541 (1)			
Er	3.758 (10)		3.432 (2)	3.532 (2)	3.574 (1)			3.527 (1)			3.364 (25)
Tm	3.749 (10)		3.414 (2)	3.516 (2)	3.562 (1)			3.516 (1)			
Yb											
Lu	3.727 (10)				3.536 (1)			3.488 (1)			3.325 (25)

phases in some of the alloys not yet investigated. The new CsCl phases found are described in Section III of this thesis. The second purpose of the present work was a systematic study of the electrical resistivity of the CsCl phases involving Cu, Ag, and Au elements. These measurements lead to the determination of the magnetic transition temperatures in these alloys. These results are described in Section IV, and discussed in Section V. In Section VI, an attempt is made to explain the electrical properties of CsCl phases involving rare earth elements. The model used takes into account the indirect exchange interaction of the 4f electrons of the rare earth ions.

II. ALLOYS INVESTIGATED AND EXPERIMENTAL TECHNIQUES

All the alloys investigated contained 50 at. % rare earth element and 50 at. % of the other metal. They included most of the rare earths with elements of the II A, I B, II B, and III A columns of the periodic table. The systems studied are summarized in TABLE 2.

Since rare earth elements cannot be obtained with extreme purity, it is important to give details about their estimated purity as well as their source of supply. This is summarized in TABLE 3. In general the rare earth metals were of purity greater than 99.9% and the other metals exceeded the 99.99% purity level.

The alloys were melted by induction heating in tantalum crucibles under an argon atmosphere. Because of the high cost of pure rare earth metals, the weight of each melt was limited to two to three grams. Chemical analyses were not performed after melting, but the small weight losses after melting, gave reliability to the assumption that the final composition was very close to the nominal one based on the weight of the components. Each alloy was melted at least twice to insure homogeneity of the melt. During heating of the mixtures of metals involving copper, silver and gold, a very strong exothermic reaction was noticed (increasing in intensity in the sequence Cu, Ag, and Au) which is an indication of the stability of the CsCl phase in these systems. For alloys involving the rare earth elements with Mg, Al, Zn, Cd, In, and Tl, the exothermic reaction was so strong that the mass was ejected from

TABLE 2

Alloys Studied in This Investigation

50 at% M / RM / R	IB			IIB			IIIA		
	Cu	Ag	Au	Zn	Cd	Hg	Al	In	Tl
Y			o	o					
La			o						
Ce			o						
Pr			o	o					
Nd			o	o					
Sm	o	o	o	o	o			o	
Eu	o	o	o	o	o	o		o	
Gd	o	o	o	o	o		o	o	o
Tb	o	o	o	o	o		o	o	o
Dy	o	o	o	o	o		o	o	o
Ho	o	o	o	o	o		o		
Er	o	o	o	o			o		
Tm	o	o	o	o			o		
Yb	o	o	o	o	o	o	o	o	o

TABLE 3

Impurity Analysis of The Elements Used in This Study

Elements	Supplied by	Purity Specification
Cu	Johnson, Matthey & Co.	Spectrographic method, Fe, 2; Pb, 2; Ni, 1; Ag, 1; Cd, Mg, Mn, Si, 1 ppm.
Ag	Engelhard Industry Inc.	99.99% Ag.
Au	Wildberg Bros. Smelting & Refining Co.	Chemical purity of 99.99% Au.
Zn	American Smelting & Refining Co.	Spectrographic method, Sb, Tl, Mn, Pb, Sn, Cr, Fe, Ni, Bi, Al, Ca, In, Ag are all none detected; Mg, 0.0001; Si, 0.0001; Cu, 0.001; Cd, 0.0003; 99.999% Zn.
Cd	American Smelting & Refining Co.	Spectrographic method, Sb, Tl, Mn, Sn, Cr, Ni, Al, Ca, In, Zn, Ag are all none detected; Mg, 0.0001; Pb, 0.0002; Si, 0.0001; Cu, 0.0001; 99.999% Cd.
Hg		99.9% Hg.
In	American Smelting & Refining Co.	Spectrographic method, Al, Tl, Ni, Bi, Zn, Sb, Ag, As, Te are all none detected; Fe, Sn are 0.0001; Pb, 0.0001; Cd, 0.0001; 99,999% In.
Tl	American Smelting & Refining Co.	Spectrographic method, Sb, Mn, Pb, Sn, Cr, Ni, Al, Ca, In, Cd, Zn are all none detected; Mg, 3 ppm; Si, Fe, Ag are less than 1 ppm; Cu, 1 ppm; Bi, 5 ppm; 99.999% Tl.
Al	Johnson, Matthey & Co.	Spectrographic method Mg, 30 ppm; Fe, 5 ppm; Si, 3 ppm; Cd, 2 ppm; Cu, 1 ppm; Na, 1 ppm; Ag, 1 ppm.

TABLE 3 (continued)

Elements	Supplied by	Purity Specification
Y	Michigan Chemical Corporation	Yb, 100 ppm; Gd, 1000 ppm; Si, 50 ppm; Ca, 100 ppm; Fe, 500 ppm; Cu, 10-100 ppm; Ta, 3400 ppm; O_2, 2900 ppm; Er, Ho, Dy, Tb, Al are not detected.
La	Michigan Chemical Corporation	Emission Spectrographic method, Ca, 100 ppm; Fe, 200 ppm; Cu, 100 ppm; Ta, 100 ppm; O_2, 1500 ppm; Pr, Ce, Si, Ni, Al are not detected.
Ce	American Potash & Chemical Corporation	Fe, 0.01%; O_2, 0.2%; other rare earth 0.1%.
Pr	American Potash & Chemical Corp.	Ta, 0.01%; Fe, 0.005%; O_2, 0.4%; other rare earth elements 0.1%.
Nd	Michigan Chemical Corporation	Emission Spectrographic method, Eu, Sm, Pr, Ce, Ta are not detected; Si, 100 ppm; Ca, 2000-5000 ppm; O_2, 570 ppm; Fe, 200 ppm; Ni, 200 ppm; Al, 200 ppm.
Sm	American Potash & Chemical Corp.	99.9% pure Sm with respect to other rare earth elements.
Eu	Michigan Chemical Corporation	Emission Spectrographic method, Si, 200 ppm; Ca, 200 ppm; Fe, 100-200 ppm; Cu, 100 ppm; Ni, 100 ppm; Al, 100 ppm; O_2, 3640 ppm; Y, Tb, Gd, Sm, Nd, La, Ta are not detected.
Gd	Atomic Energy Commission	99.9% pure Gd.
Tb	American Potash & Chemical Corp.	Ta, 0.001%; Fe, 0.001%; O_2, 0.01%; Y, 0.005%; Dy, 0.01%; other rare earth elements 0.1%.

TABLE 3 (continued)

Elements	Supplied by	Purity Specification
Dy	American Potash & Chemical Corp.	Ta, 001%; Ca, 0.02%; Fe, 0.015%; O_2, 0.2%; other rare earth elements, 0.1%.
Ho	American Potash & Chemical Corp.	Ta, 0.001%; Ca, 0.02%; Fe, 0.001%; O_2, 0.25%; other rare earth elements, 0.1%.
Er	American Potash & Chemical Corp.	O_2, 0.4000%; N_2, 0.0045%; other rare earth elements, 0.1%.
Tm	American Potash & Chemical Corp.	Ta, 0.001%; Mg, 0.0005%; Fe, 0.0001%; N_2, 0.039%; O_2, 0.49%.
Yb	Michigan Chemical Corporation	Emission Spectrographic method, Lu 100 ppm; Tm, Er, Ta are not detected; Si, 2000-5000 ppm; Ca, 200 ppm; Fe, 200-2000 ppm; Cu 100 ppm; Ni, 100 ppm; Al, 2000 ppm; O_2, 1500 ppm.

the open tantalum crucible. These alloys were prepared by enclosing the constituents into a tantalum tube (0.95 cm OD and about 5 cm long) sealed at both ends by spot welding and heating this tube by induction under an argon atmosphere. The same procedure was used for rare earth compounds with mercury, in order to avoid volatilization of mercury. In all cases, the rate of heating of the components by induction was maintained below a certain limit to avoid an explosive reaction.

After melting, some additional precautions had to be taken to prevent reaction with air. The alloys of rare earths with Cu, Ag, Au, Al, Mg were stable in air. The Zn alloys were also stable with the exception of YbZn. Rapid reaction with air occurred in alloys with Cd, Hg, In, and Tl and YbCd which ignited spontaneously in air. All these alloys were handled in a dry box for preparing powders which were sealed into capillaries for X-ray diffraction analysis. Alloys containing Cu, Ag, and Au were also rapidly quenched from the liquid state, as reported in references (1) and (2).

The structure of the alloys was determined by the Debye-Scherrer method, using a 114.6 mm diameter camera and copper Kα radiation with a Nickel filter. Lattice parameters were computed using the Nelson-Riley extrapolation. The accuracy of these parameters, however, varied greatly from alloy to alloy depending on the sharpness of the back reflection lines, and the uncertainties involved were estimated in each case. The reliability in establishing the existence of a CsCl structure rather than a random body-centered structure is directly related to the difference in the atomic scattering

factors of the rare earth metal and the other elements. In some cases, for which this difference was small, the CsCl structure superlattice lines were so faint that the CsCl structure could not be firmly established, but appeared to be the most probable one.

III. NEW CSCL PHASES

A. LATTICE PARAMETER MEASUREMENTS

A complete list of the CsCl phases found during this investigation is given in TABLE 4 together with their lattice parameters. Some of these results have been reported by the author in published papers and references are given in the table. Since some of these phases were obtained only by fast cooling from the liquid state, special symbols are used in TABLE 4 to indicate if the CsCl phases can be obtained by slow cooling, or only by rapid quenching from the liquid state. In general if the phase exists after slow cooling, it also exists after rapid cooling.

The absence of lattice parameter values in the double entry TABLE 4 does not mean that all these alloys were excluded from the present investigation, but rather that the CsCl structure was not found after either slow cooling or rapid quenching. In YbAg, some diffraction lines could be attributed to a CsCl phase, but there were too many other diffraction peaks to exclude the possibility of a more complex phase. The same situation occured in the case of YbAu. The AuCe and AuLa alloys did not show the CsCl structure after slow cooling, and it was anticipated that they would yield that structure under rapid quenching conditions since they would nicely complete the Au series. These alloys could not be quenched from the liquid state because they were too rapidly oxidized and the rapid cooling apparatus, in its present form, does not provide adequate atmosphere protection. Alloys of Eu with Zn and Cd were prepared,

TABLE 4

Lattice Parameters of Intermediate Phases with CsCl Type Crystal Structure Involving Rare Earth Elements

	Cu[2]	Ag[1]	Au[1]	Zn[2]	Cd(#)	Hg(#)	In(#)	Tl(#)
Y			3.559±2	3.577±3	3.722±2			
La								
Ce								
Pr			3.68±1 (δ)					
Nd			3.659±4 (δ)	3.667±2				
Sm	3.528±2(δ)	3.673±3	3.621±2 (δ)	3.627±1				
Eu			▽(#)	▽(#)	▽	▽		3.975±3
Gd			3.593±2 (δ)	3.602±4	3.755±3			Δ
Tb	3.480±4	3.625±3	3.576±2	3.576±4	Δ			Δ
Dy	3.460±3		3.555±2	3.563±3	Δ			Δ
Ho	3.445±1	3.592±3	3.541±1	3.547±3	3.701±2			Δ
Er		3.574±2	3.527±2	3.532±3	3.685±1			Δ
Tm	3.414±1	3.562±2	3.516±3	3.516±3				Δ
Yb	▽(#)	▽(#)	▽(#)	3.629±1(#)	3.8086±5	3.735±2	3.808±1	3.828±4

(#) Not previously reported.

(Δ) Alloy was studied and CsCl type structure detected, but X-ray pattern was too diffuse for parameter measurements.

(▽) Alloy was studied but no CsCl type structure was found.

(δ) CsCl type structure was obtained only by rapid quenching from liquid state.

but did not show a CsCl structure after slow cooling. In the Cd column, the presence of a CsCl phase was detected in alloys with Tb and Dy, but no lattice parameter is reported in TABLE 4 because of the very diffuse reflections on the X-ray pattern. An alloy of Eu with Hg was also prepared but did not show a CsCl structure. In the In column, alloys were prepared with Sm, Gd, Tb, Dy and Ho, but no definite evidence of a CsCl structure was found.

For alloys of Tl with rare earth elements, the EuTl and YbTl alloys show clearly the CsCl type structure, and the lattice parameters are given. However for alloys with Gd, Tb, Dy, Ho and Er the X-ray patterns were too diffuse and no quantitative data was obtained. Only slowly cooled alloys of this group were studied, because they were too reactive to be rapidly cooled from the melt.

A search for CsCl phase was also made in binary alloys of rare earth with aluminum (not listed in TABLE 4). From the published phase diagrams of Al with La, Ce, Pr, and Y,[3] it is known that the CsCl phase in these systems forms by peritectic reaction. For rare earth heavier than Nd, the phase diagrams are not known, and alloys were prepared with Gd, Tb, Dy, Ho, Er, Tm, and Yb. No CsCl was detected either in the slowly cooled alloys or in those rapidly cooled from the melt. Instead, the X-ray diffraction patterns showed the presence of a $MgCu_2$ type phase (C15 type). It is probable that in these systems, the $MgCu_2$ phase is a very stable congruent melting phase; and without special care in promoting the formation of an hypothetical CsCl phase formed by peritectic reaction at lower temperature, the as-cast alloys (and a fortiori the rapidly

cooled ones) will contain the $MgCu_2$ phase.

B. CORELATION BETWEEN LATTICE PARAMETERS AND TRIVALENT IONIC RADII

In previous investigations of the CsCl type phases involving rare earth elements, it was pointed out that a linear relationship exists between the lattice parameters of these phases and the radii of the trivalent rare earth ions. This relationship was first pointed out by Iandelli[4] and additional evidence was presented in references (1) and (2).

In the CsCl type crystal structure, the lattice parameter, a, corresponds to the distance between any two nearest neighboring atoms of the same kind. $\sqrt{3}a/2$ is the distance between any two nearest neighboring atoms of different kinds. The relation

$$\sqrt{3}a = 2r_E + 2r_M$$

exists if the atoms or the ions are assumed in sphere contact alone the body diagonal direction of the unit cell of the lattice. r_E and r_M are the atomic or ionic radii of rare earth element and the other element respectively.

The r_M values were determined for each phase and the results are presented in TABLE 5. It can be seen that the r_M values for a given M are constant within experimental uncertainties and the average value is also listed in TABLE 5. These results indicate that a given metal in the CsCl structure with any rare earth element has a "constant radius" under the assumption that the lattice parameter, a, is either larger than or equal to twice the value of this "constant radius." From TABLE 5, it is clear that the lattice

TABLE 5

Characteristic Values for CsCl Phases Involving Rare Earth Elements

Phases	r_E	a	$a\sqrt{3}/2$	r'_M	
YAg	0.91	3.617	3.132	2.222	
LaAg	1.061	3.781	3.273	2.213	
CeAg	1.034	3.746	3.132	2.210	
PrAg	1.013	3.739	3.238	2.225*	
NdAg	0.995	3.714	3.216	2.221	
SmAg	0.964	3.673	3.181	2.217	
GdAg	0.938	3.6476	3.1589	2.221	
TbAg	0.923	3.625	3.139	2.216	
DyAg	0.908	3.608	3.125	2.217	
HoAg	0.894	3.592	3.111	2.217	
ErAg	0.881	3.574	3.095	2.214	
TmAg	0.869	3.562	3.085	2.216	$r_M = 2.215 \pm 5$
YAu		3.559	3.082	2.172	
PrAu		3.68	3.187	2.174	
NdAu		3.659	3.169	2.172	
SmAu		3.621	3.136	2.174	
GdAu		3.593	3.112	2.174	
TbAu		3.576	3.097	2.171	
DyAu		3.555	3.079	2.173	
HoAu		3.541	3.067	2.173	
ErAu		3.527	3.054	2.173	
TmAu		3.516	3.045	2.176	$r_M = 2.172 \pm 2$
YCu		3.476	3.010	2.100*	
SmCu		3.528	3.055	2.090	
GdCu		3.505	3.035	2.097*	
TbCu		3.480	3.014	2.091	
DyCu		3.460	2.996	2.088	
HoCu		3.445	2.983	2.089	
ErCu		3.432	2.972	2.091	
TmCu		3.414	2.957	2.091	$r_M = 2.090 \pm 2$

TABLE 5 (continued)

Phases	r_E	a	$a\sqrt{3}\frac{1}{2}$	r_M	
YZn		3.577	3.098	2.188	
LaZn		3.759	3.255	2.194*	
CeZn		3.704	3.208	2.174	
PrZn		3.678	3.185	2.172	
NdZn		3.667	3.176	2.181	
SmZn		3.627	3.141	2.177	
GdZn		3.602	3.119	2.181	
TbZn		3.576	3.097	2.174	
DyZn		3.563	3.086	2.178	
HoZn		3.547	3.072	2.178	
ErZn		3.532	3.059	2.178	
TmZn		3.516	3.045	2.176	$r_M = 2.178 \pm 2$
YbZn		3.629	3.143		
YCd		3.722	3.223	2.310	
LaCd		3.905	3.382	2.321	
CeCd		3.865	3.347	2.313	
PrCd		3.830	3.317	2.304*	
NdCd		3.811	3.300	2.305*	
SmCd		3.771	3.266	2.302*	
GdCd		3.755	3.251	2.313	
HoCd		3.701	3.205	2.311	
ErCd		3.685	3.191	2.310	$r_M = 2.310 \pm 5$
LaHg		3.845	3.330	2.269	
CeHg		3.816	3.305	2.271	
PrHg		3.799	3.290	2.276	
NdHg		3.780	3.273	2.278	
SmHg		3.744	3.242	2.278	
TbHg		3.678	3.185	2.261*	$r_M = 2.275 \pm 5$
YbHg		3.735	3.235		
LaTl		3.922	3.396	2.335	
CeTl		3.893	3.371	2.337	
PrTl		3.869	3.350	2.337	
SmTl		3.813	3.302	2.338	$r_M = 2.336 \pm 2$
YbTl		3.828			
EuTl		3.975			

TABLE 5 (continued)

Phases	r_E	a	$a\sqrt{3}\frac{1}{2}$	r'_M	
YMg		3.80	3.291	2.38	
LaMg		3.967	3.435	2.374	
CeMg		3.899	3.377	2.343*	
PrMg		3.888	3.367	2.351*	
NdMg		3.867	3.349	2.354*	
SmMg		3.810	3.299	2.335*	
GdMg		3.824	3.312	2.374	
TbMg		3.796	3.287	2.364	
DyMg		3.786	3.272	2.364	
HoMg		3.776	3.270	2.376	
ErMg		3.758	3.254	2.373	
TmMg		3.749	3.247	2.378	$r_M = 2.370 \pm 5$
LuMg		3.727	3.288		

(*) Not included for calculating the average value r_M (see TABLE 1).

parameters, a, are definitely smaller than their corresponding $2r_M$ value for every M metal, therefore the r_M is considered as a characteristic value other than the radius for the M metal in CsCl phases with rare earth elements. If in addition, the lattice parameter of the CsCl phases varies linearly with the rare earth trivalent ionic radius, it must follow an equation of the type

$$\sqrt{3}a = 2r_E + K \qquad (1)$$

in which the constant K is equal to $2r_M$. All the lattice parameters measurements of CsCl phases obtained in this study (with the exception of those involving In, Al and Rh, for which too few alloys were studied) are plotted vs. the trivalent ionic radius of the rare earth metal. In Fig. 1 the solid straight lines shown on the graph were traced so that their interception with the vertical axis was equal to the average value for $(2/\sqrt{3})r_M$ (shown in TABLE 5) and their slope was equal to $2/\sqrt{3}$. The relatively good fit between the experimental data and the linear relationship confirms the previously published results on a limited number of phases, and demonstrate that the lattice parameter of the CsCl phases involving rare earth elements is a linear function of the trivalent ionic radius of the rare earth element.* So far, however, no theoretical quantitative explanation has been found for this general rule.

A consequence of the validity of equation (1) is that the parameter r_M associated with the metallic element entering into a

---

* The data points in Figure 1 marked with arrows, do not represent reliable results (See TABLE 5)

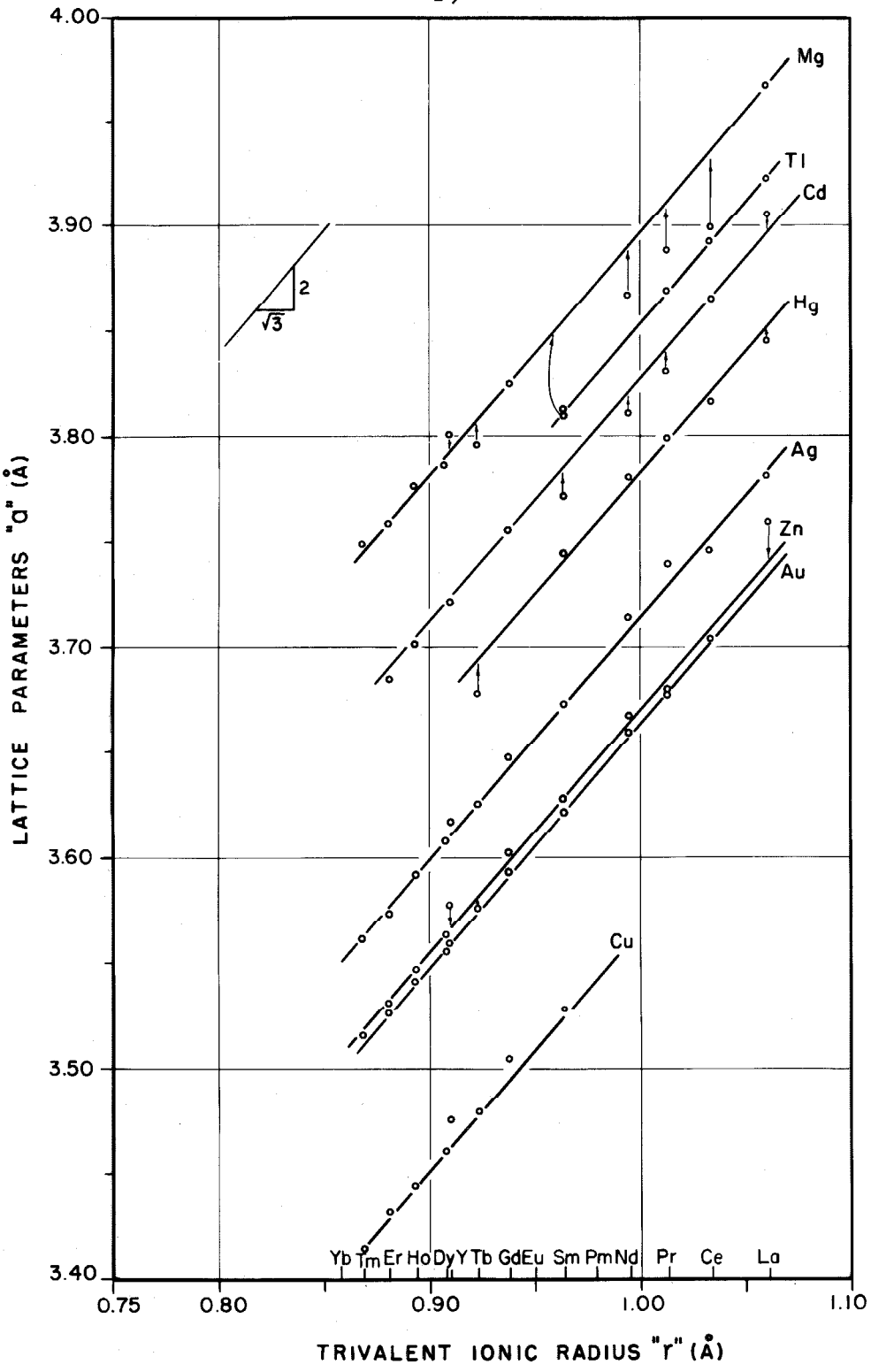

Fig. 1. Relationship between The Trivalent Ionic Radii of Rare Earth Elements and The Lattice Parameters of CsCl Phases

CsCl structure with a rare earth element is a constant and is not influenced by the nature of the rare earth metals. In addition, this parameter is in all cases much larger than the generally accepted radius of the element in its own crystal structure. A comparison between the elemental radius and the parameter present in the CsCl structure is given in TABLE 6. The percentage increase in diameter is not constant and varies from about 32 to 39%.

With increasing size of the elemental radii, the CsCl lattice parameters of a given rare earth element should increase in the order of Cu, Zn, Au, Ag, Cd, Hg, Tl, and Mg. Instead the order is Cu, Au, Zn, Ag, Hg, Cd, Tl, and Mg. The only two pairs out of order are due to Au and Hg having smaller radii than expected. No explanation has been found for this rather strange behavior, but in general, the larger the difference between the electronegativities of the two components of an intermediate phase the stronger is the stability of that phase. Hence the lattice parameters of a phase between two elements having a large difference in electronegativity should be, in general, smaller than those of phases for which the difference in electronegativity is small. The electronegativity of Cu, Zn, Au, ... etc. and values of $\Delta n = n_M - \bar{n}_E$, (where $\bar{n}_E$ is the average value of the electronegativity of rare earth element and is taken as 1.2) are shown in TABLE 7 for comparison. From an elementary point of view based on the above arguments, the lattice parameters of the CsCl phases should increase in the order of Au, Cu, Ag, Hg, Tl, Cd, Zn, and Mg if the electronegativity effect dominates. Comparing this fact and the size effect with the experimental results,

TABLE 6

Radii (Atomic and Ionic) and Electronegativity of the Metals in CsCl Phases

	Characteristic value r_M (Å)	Pauling's Atomic Radius r'_M (Å)	$\frac{r_M - r'_M}{r_M}$ %	Pauling's Electronegativity n_M	$\Delta n = n_M - \bar{n}_E$ *
Cu	2.090	1.277	38.9	1.9	~ 0.7
Zn	2.178	1.339	38.5	1.6	~ 0.4
Au	2.172	1.439	33.8	2.4	~ 1.2
Ag	2.215	1.441	34.9	1.9	~ 0.7
Cd	2.310	1.508	34.7	1.7	~ 0.5
Hg	2.275	1.512	33.5	1.9	~ 0.7
Tl	2.336	1.596	31.7	1.8	~ 0.6
Mg	2.370	1.600	32.5	1.2	~ 0.0

* $\bar{n}_E$, average electronegativity of rare earth elements, which is about 1.2.

it appears that in the phases of RCu, RZn, RAg, and RTl the size effect dominates the "a" value but the electronegativity effect dominates the phases of RAu, RHg, RCd, while both effects have caused large lattice parameters in RMg phases.

The lattice parameters of the CsCl phases in alloys involving Ytterbium (listed in TABLE 7), were not considered in the previous discussion because they did not fit on the corresponding straight lines when plotted vs. the trivalent ionic radius of Yb. The lattice parameter of the only Europium alloy studied (EuTl) was not considered because it did not fall in line with the other Tl alloys. However, if we assume a linear relationship for compounds involving Yb and Eu, the ionic radius of Yb in the compounds would be about 0.97 ± 1 Å and that of Eu in EuTl about 1.11 ± 1 Å. This would correspond to a valence of 2.2 ± 1 for both Yb and Eu ions. (The trivalent radius of Yb is 0.858 Å and that of Eu is 0.950 Å; the divalent radius of Yb is 1.02 Å and that of Eu is 1.137 Å). It is not surprising that among the rare earth metals, Eu and Yb could exhibit different properties since these are the only two rare earth metals that have anomalous behavior in their atomic radii.

TABLE 7

Lattice Parameters of CsCl Phases

	Mg	Tl	In	Cd	Hg	Ag	Al	Zn	Au	Cu	Rh
Eu		3.975									
La	3.967	3.922		3.905	3.845	3.781	3.79	3.759			
Ce	3.899	3.893		3.865	3.816	3.746		3.704			
Pr	3.888	3.869		3.830	3.799	3.739		3.678	3.68		
Nd	3.867			3.811	3.780	3.714	3.74	3.667	3.659		
Yb		3.828	3.808	3.8060	3.735			3.629			
Sm	3.810	3.813		3.771	3.744	3.673		3.627	3.621	3.528	
Gd	3.824			3.755		3.6476		3.602	3.593	3.505	
Tb	3.796				3.678	3.625		3.576	3.576	3.480	
Y	3.80			3.722		3.617		3.577	3.559	3.476	3.41
Dy	3.786					3.608	3.71	3.563	3.555	3.460	
Ho	3.776			3.701		3.592		3.547	3.541	3.445	
Er	3.758			3.685		3.574		3.532	3.527	3.432	3.364
Tm	3.749					3.562		3.516	3.516	3.414	
Lu	3.727										3.325
Sc											3.206

IV. ELECTRICAL RESISTIVITY OF CSCL PHASES

The electrical resistivity of the rare earth metals has been extensively studied during the last ten years.[26], [27], [28], [29], [30] For most of the rare earths, there are very pronounced anomalies in the variation of electrical resistivity with temperature which have been attributed to the interaction between the conduction electrons and the magnetic ions. An indirect exchange interaction mechanism was suggested and the electrical resistivities of binary alloys were investigated[31] in order to obtain more direct evidence for this indirect interaction. The binary CsCl type phases formed a very useful series of alloys for this purpose because of their simple crystal structure and the simple electronic configuration of the alloying element other than the rare earth. This thesis reports on additional measurements made on the electrical resistivity of CsCl phases involving eight of the rare earth metals with Cu, Ag, and Au.

A. SPECIMEN PREPARATION AND EXPERIMENTAL METHODS

The cylindrical bars (about 2 mm in diameter by about 20 mm long) required for resistivity measurements were prepared in the following manner. The alloys prepared by melting the constituents as described in Section II were powdered and the powder was tightly packed into a tantalum tube having a 2.8 mm inside diameter. The tube was sealed by spot welding and the alloy was remelted by slowly introducing the tube into the induction coil. This operation was repeated several times in an effort to eliminate gas bubbles from the cylindrical bar during solidification. After the last melting, the bar

(including the tantalum tubing) was turned in a lathe to a final diameter smaller than the original inside diameter of the tantalum tubing, in order to eliminate any outside layer that may have been contaminated by reaction with tantalum. Two potential leads made of pure platinum, and separated by a distance of about 12 mm, were spot welded to the specimen.

The resistance of the specimens was measured by means of a Leeds and Northrup type K-3 potentiometer. The standard procedure of reversing the current was used in order to minimize thermal emf in the contacts. Measurements were carried out from room temperature down to liquid helium temperature. A double dewar arrangement was designed, in which the inner dewar, having a diameter of 4 in., was immersed in liquid nitrogen contained in an outside dewar 12 in. in diameter and 16 in. deep. The specimens were inside a brass chamber, about 2.5 in. high and 2.5 in. in diameter which was immersed into the inner dewar.

Temperatures were measured by means of copper-constantan thermocouples which were calibrated against a Honeywell calibrated germanium resistor thermometer from 4.2° K to 100° K and from 100° K up to room temperature, the calibration table of Powell et. al. being used.[32] The reference temperature for the thermocouples were at boiling liquid nitrogen temperature. Thermocouples were pressed against the specimen inside the brass chamber.

In an effort to save time, four specimens were mounted in the brass cavity, and were connected in series with the constant

current supply. Eight potential leads were therefore required in connection with a suitable switching arrangement. In an effort to reduce thermal conduction through the leads, about 15 in. of extra length of each wire was coiled around the specimen and maintained within the brass chamber of low temperature.

Resistivity measurements were made while the temperature of the specimens was slowly increased. The rate of temperature rise between 4.2° K and 77° K was such that it took about eight hours to cover this temperature interval. This allowed sufficient time to perform quasi-isothermal measurements. Between 77° K and room temperature, the inner dewar (still immersed in the outer dewar filled with liquid nitrogen) was warmed by passing a constant flow of helium gas, and waiting for equilibrium temperature under constant flow conditions. Temperature readings were taken before and after each measurement and the difference between these two temperatures did not generally exceed 1° K. The total warming up time from 77° K to room temperature was of the order of thirty hours.

The uncertainties in the reported values of resistivity at a given temperature are of two kinds: the results of errors in measuring the dimensions of the specimen and errors in the electrical resistance measurement. Because of the small size of the specimen, the probable errors in the geometrical dimensions of each specimen were rather large and the uncertainties in this factor are estimated to be about within ± 2%. The electrical measurements were relatively much more accurate. The current through the specimen could be

measured less than 1 part in 10^5, and the potential was measured within 0.5μ V, or a probable error of ± 0.5%. The probable uncertainty in the electrical resistance measurements, at a given temperature is estimated to be less than 1%. The larger uncertainty in the resistivity values due to dimensional measurements (namely ± 2%) would just shift the resistivity vs. temperature curves without changing their shape. Since the conclusion of this work is concerned with the anomalies found in the resistivity-temperature curves, the uncertainty in the dimensions of the specimens is not of primary importance. As far as the temperature is concerned, it is estimated that each resistance measurement was taken within a range of temperatures not exceeding 1^{o}K.

B. RESULTS

Nineteen CsCl phases of rare earth metals with Cu, Ag, and Au were studied. These phases are shown in the double entry TABLE 8. In the table, CuEr is not listed because of failure in the making of the cylindrical specimen. The main features of the Resistivity vs. Temperature curves of the CsCl phases which are given in Fig. 2 to Fig. 20 will be briefly described.

Yttrium-Silver: The resistivity of these alloys is almost constant between 4.2°K and about 15°K. This is probably the residual resistivity. At higher temperature the curve does not show any sharp change in slope, although there is a gradual change from 0.09μΩ-cm/°K around 40°K down to 0.08μΩ-cm/°K above 70°K. YAg is probably paramagnetic down to 4.2°K. (see Fig. 2)

Neodymium-Silver: The resistivity increases rapidly

TABLE 8

CsCl Phases Used For Electrical Resistivity-Temperature Measurement

		AuGd	AuTb	AuDy	AuHo	AuEr	AuTm
AgY	AgNd	AgGd	AgTb	AgDy	AgHo	AgEr	AgTm
		CuGd	CuTb	CuDy	CuHo		CuTm

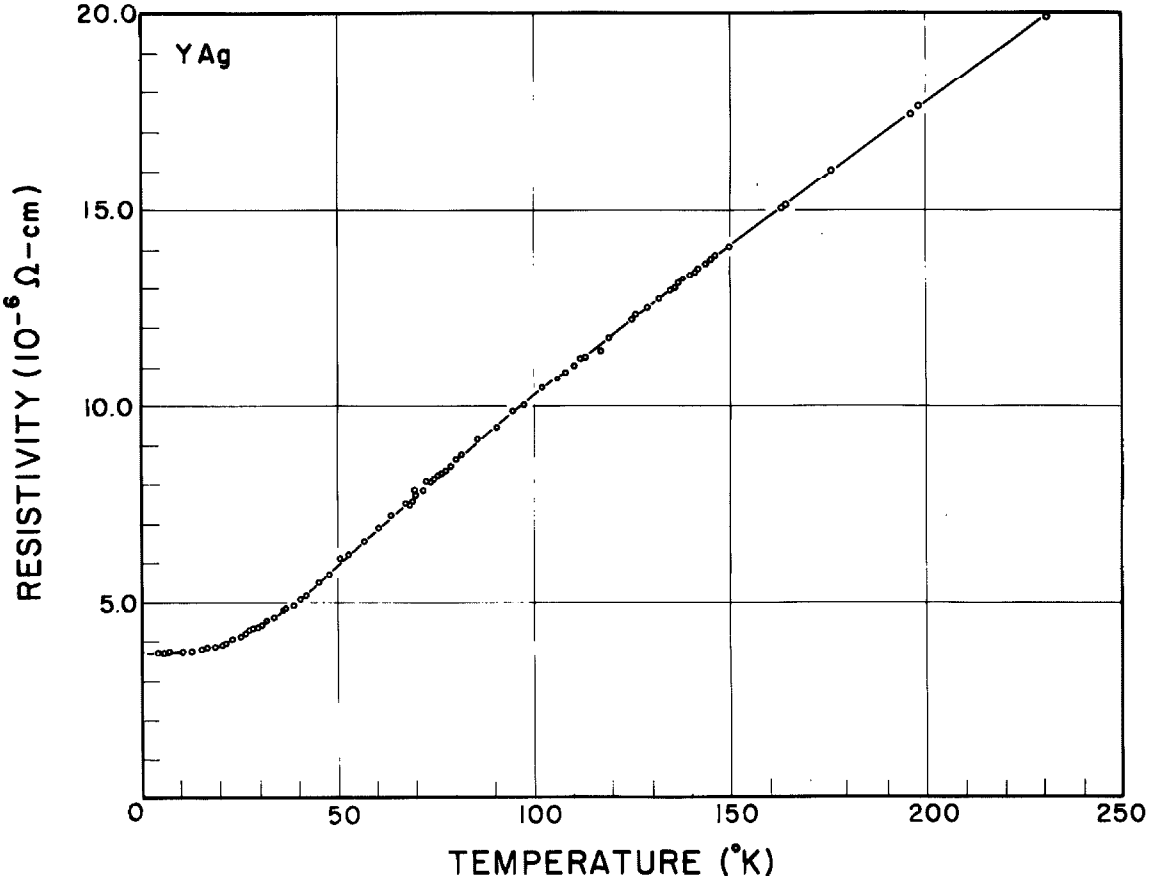

Fig. 2. Resistivity-Temperature Relationship for YAg Intermediate Phase

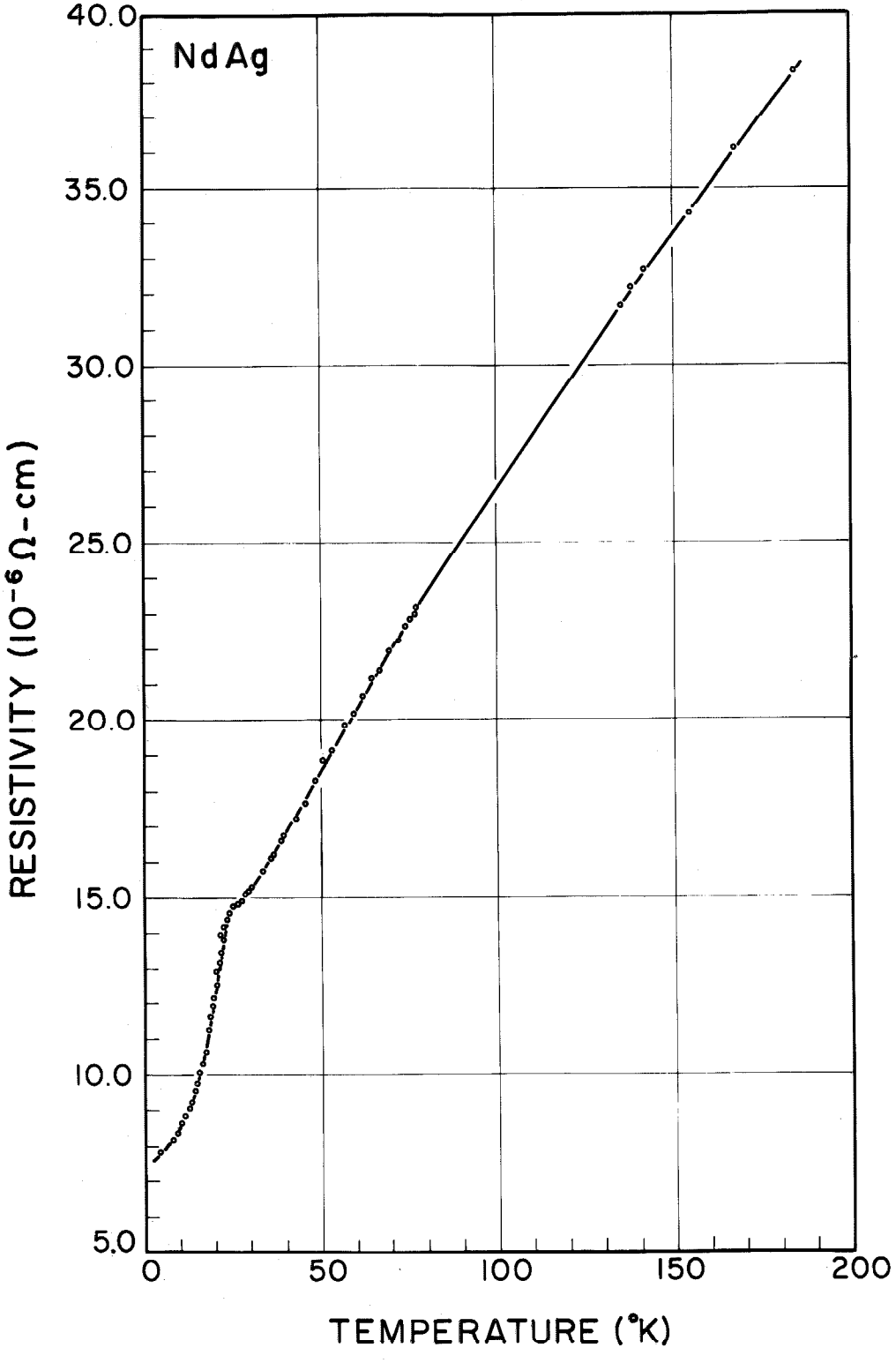

Fig. 3. Resistivity-Temperature Relationship for NdAg Intermediate Phase

between 4.2°K and about 24°K at which temperature there is a definite change of slope. The slope is very small up to 28°K, and then increases to a value of about 0.15μΩ-cm/°K. (see Fig. 3)

Gadolinium with Copper, Silver and Gold: The curves for Gd with Cu and Ag have similar characteristics with a well defined change in slope at about 135°K for Cu and about 137°K for Ag. For Au, the resistivity remained practically constant from 42°K to about 50°K with a drastic change in slope across this transition. (see Fig. 4, 5, 6)

Terbium with Copper, Silver and Gold: These three phases showed a progressive but definite change in slope. (see Fig. 7, 8, 9)

Dysprosium with Copper, Silver and Gold: All these phases showed a well-defined change in slope within a narrow temperature range. (see Fig. 10, 11, 12)

Holmium with Copper, Silver and Gold: Around the transition temperature, the slope of the resistivity temperature curve drops to a low value before it increases again to a constant value. (see Fig. 13, 14, 15)

Erbium and Thulium with Copper, Silver and Gold: In all these alloys the slope of the resistivity-temperature curve reaches practically zero in the transition range before it progressively increases to a constant value. (see Fig. 16, 17 for ErAg, ErAu and 18, 19-1, 19-2, 20-1, 20-2 for TmCu, TmAg, and TmAu)

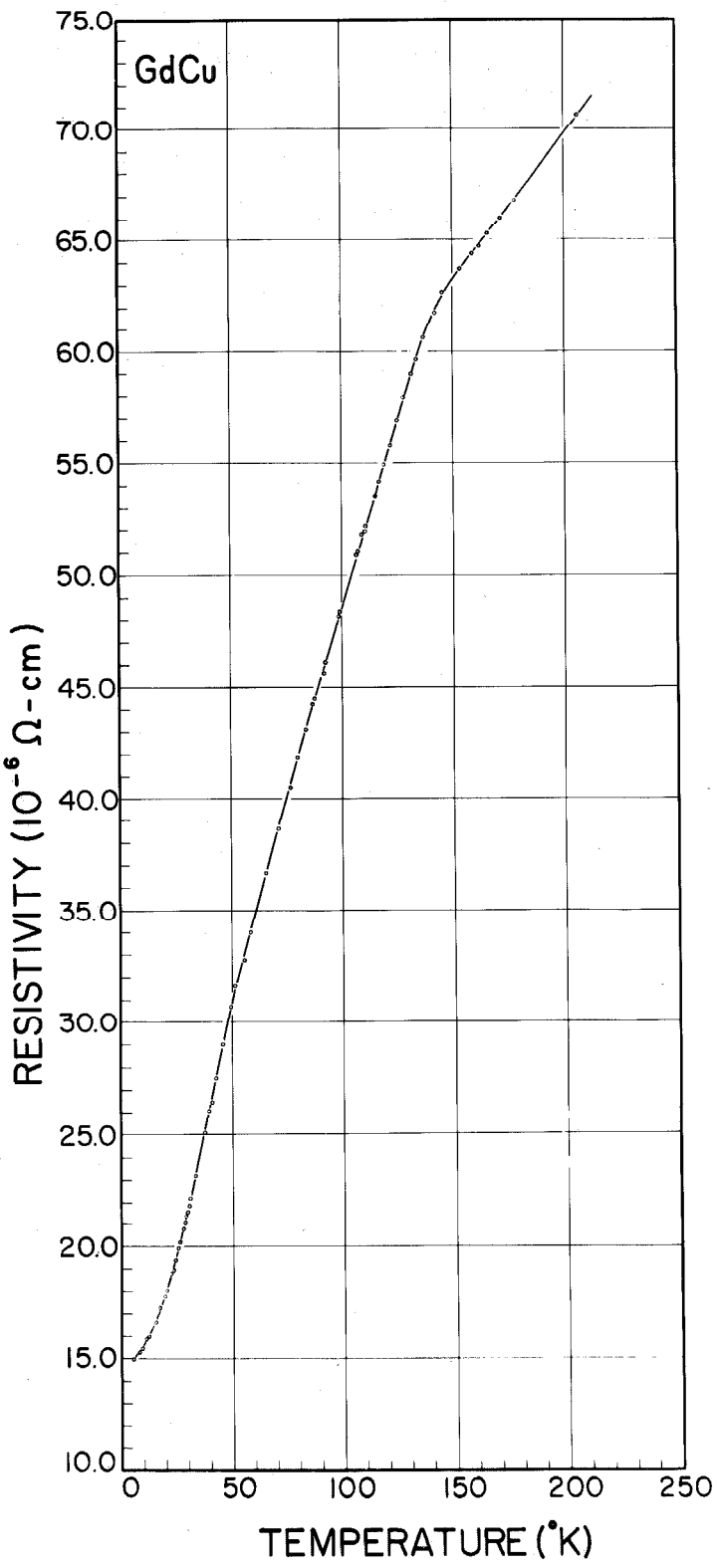

Fig. 4. Resistivity-Temperature Relationship for GdCu Intermediate Phase

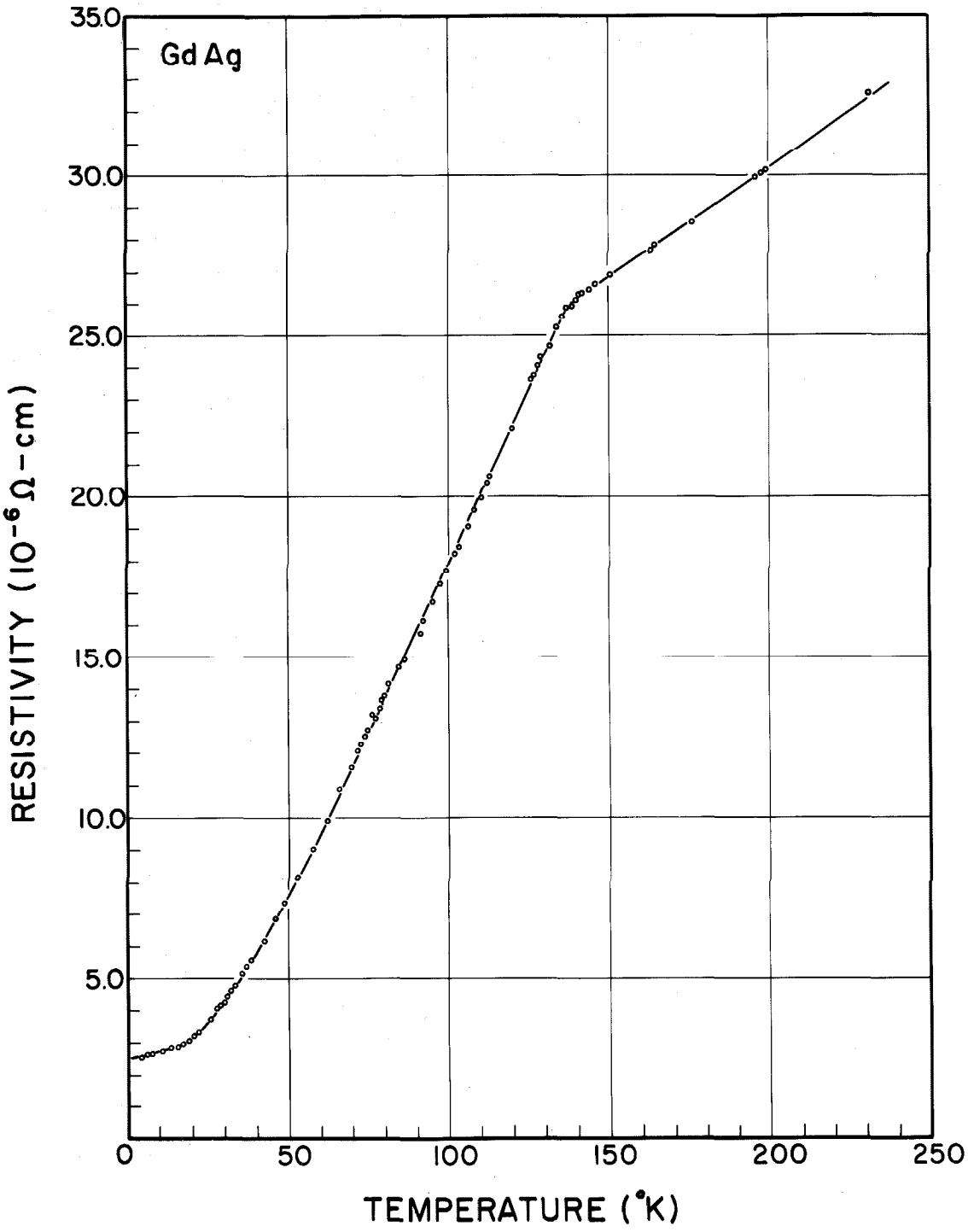

Fig. 5. Resistivity-Temperature Relationship for GdAg Intermediate Phase

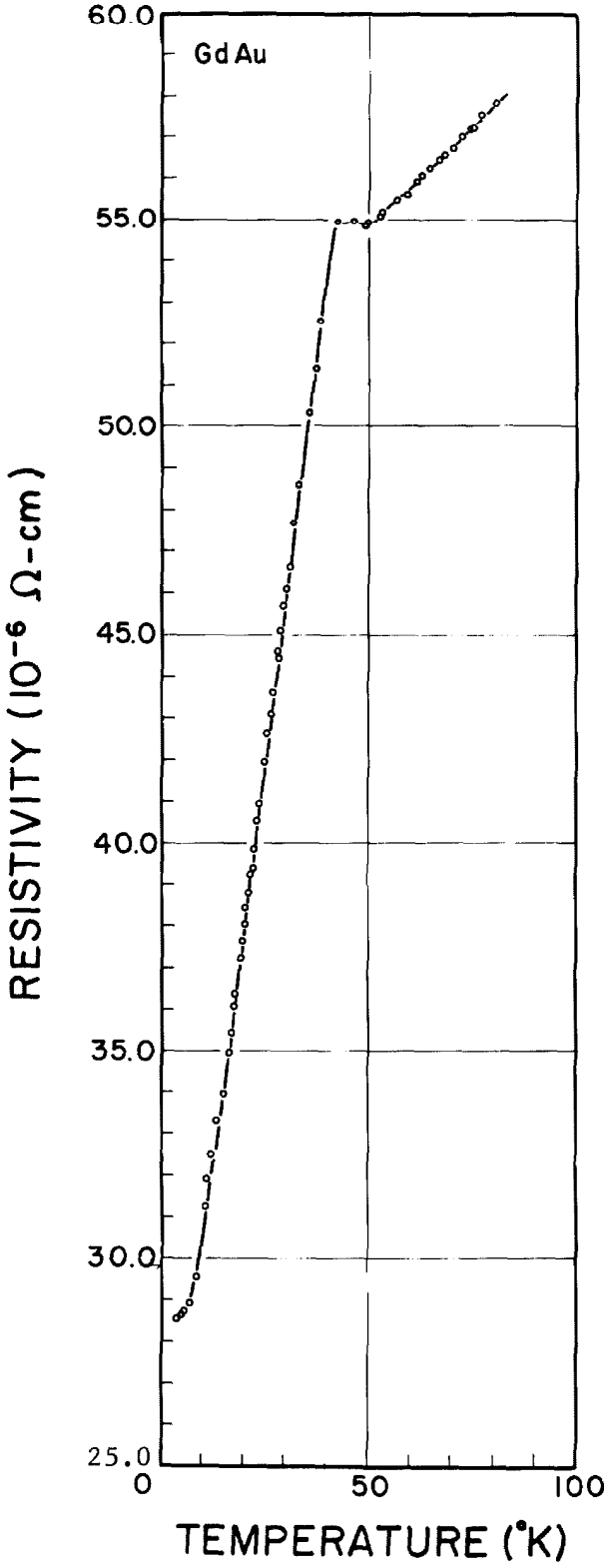

Fig. 6. Resistivity-Temperature Relationship for GdAu Intermediate Phase

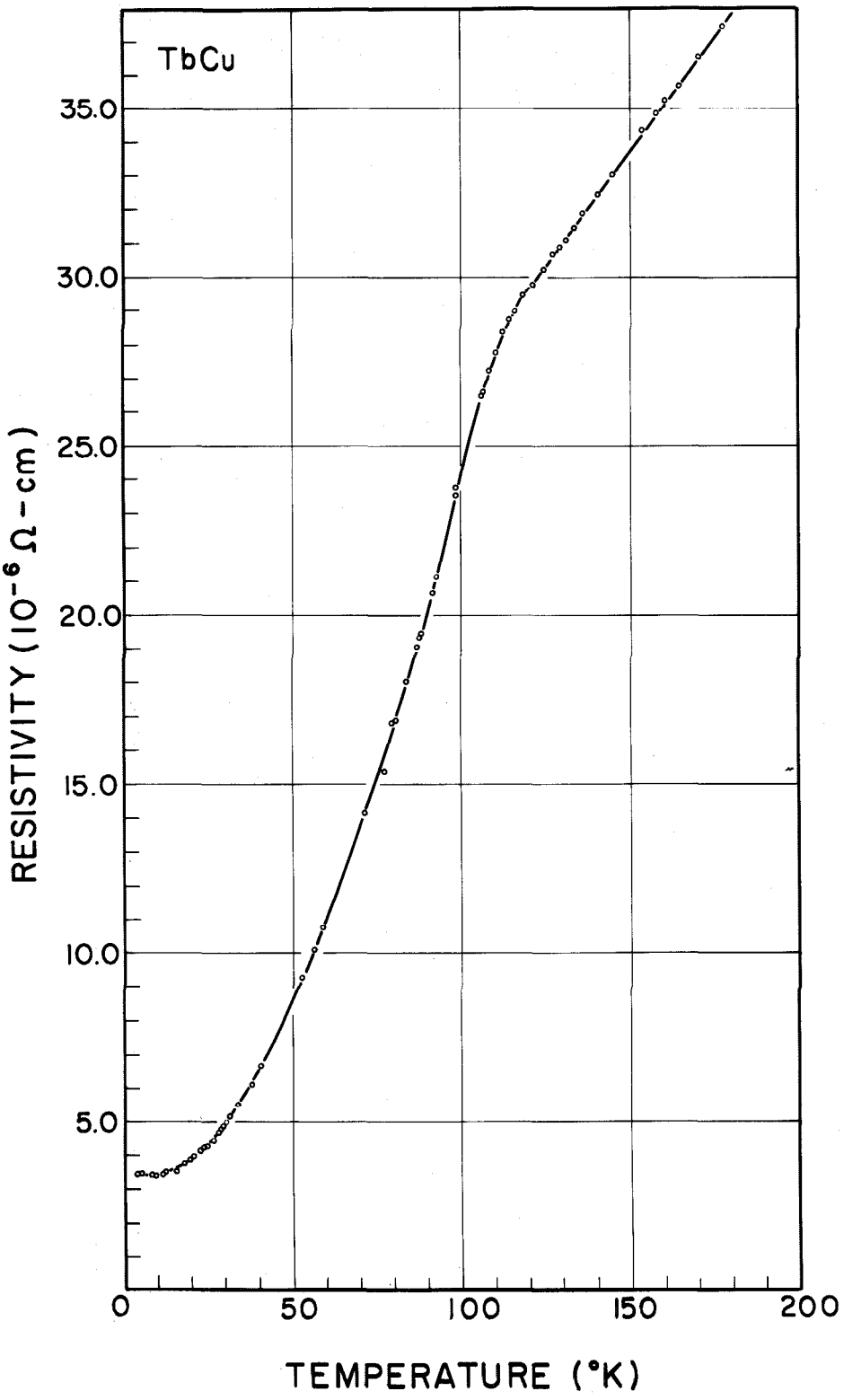

Fig. 7. Resistivity-Temperature Relationship for TbCu Intermediate Phase

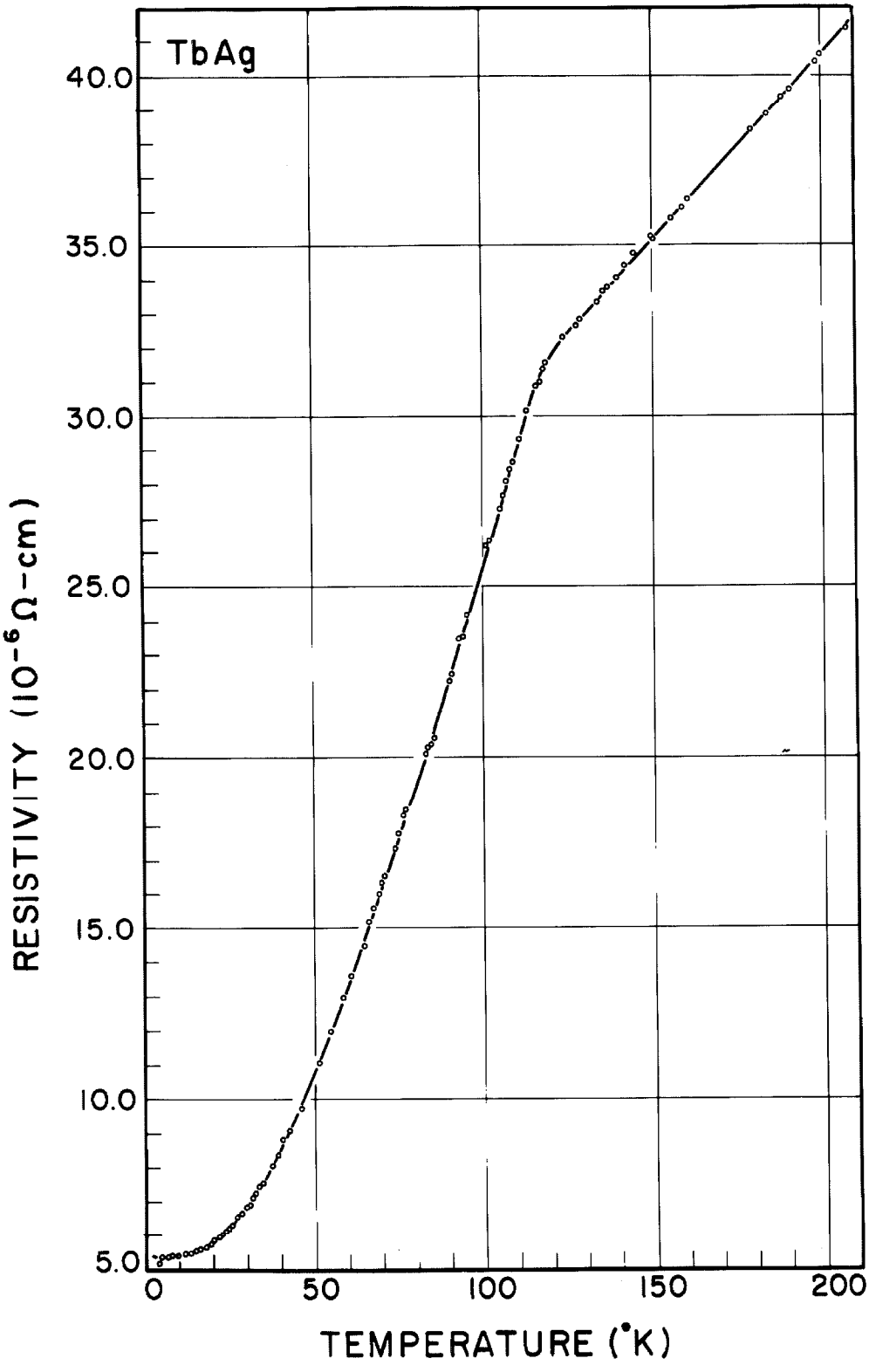

Fig. 8. Resistivity-Temperature Relationship for TbAg Intermediate Phase

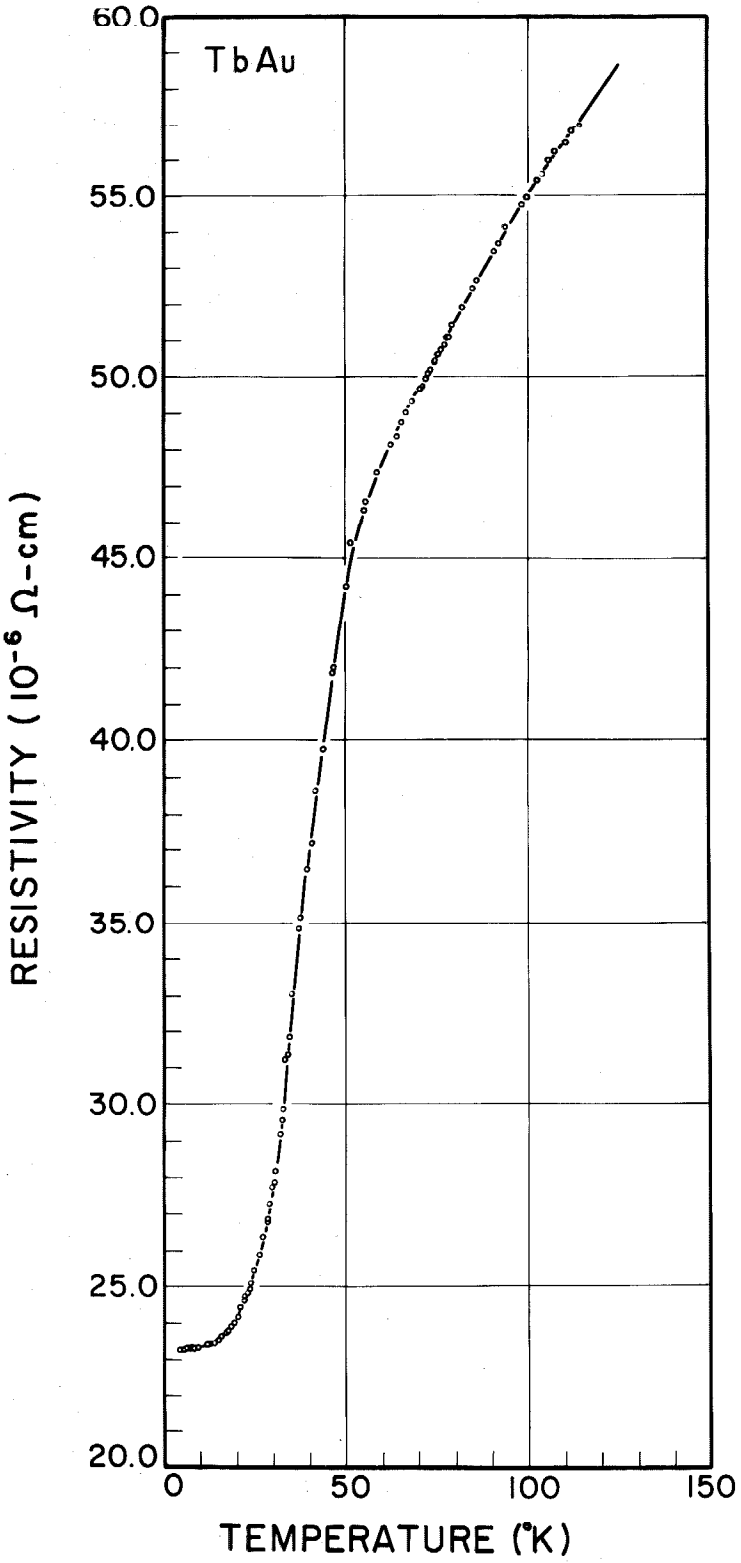

Fig. 9. Resistivity-Temperature Relationship for TbAu Intermediate Phase

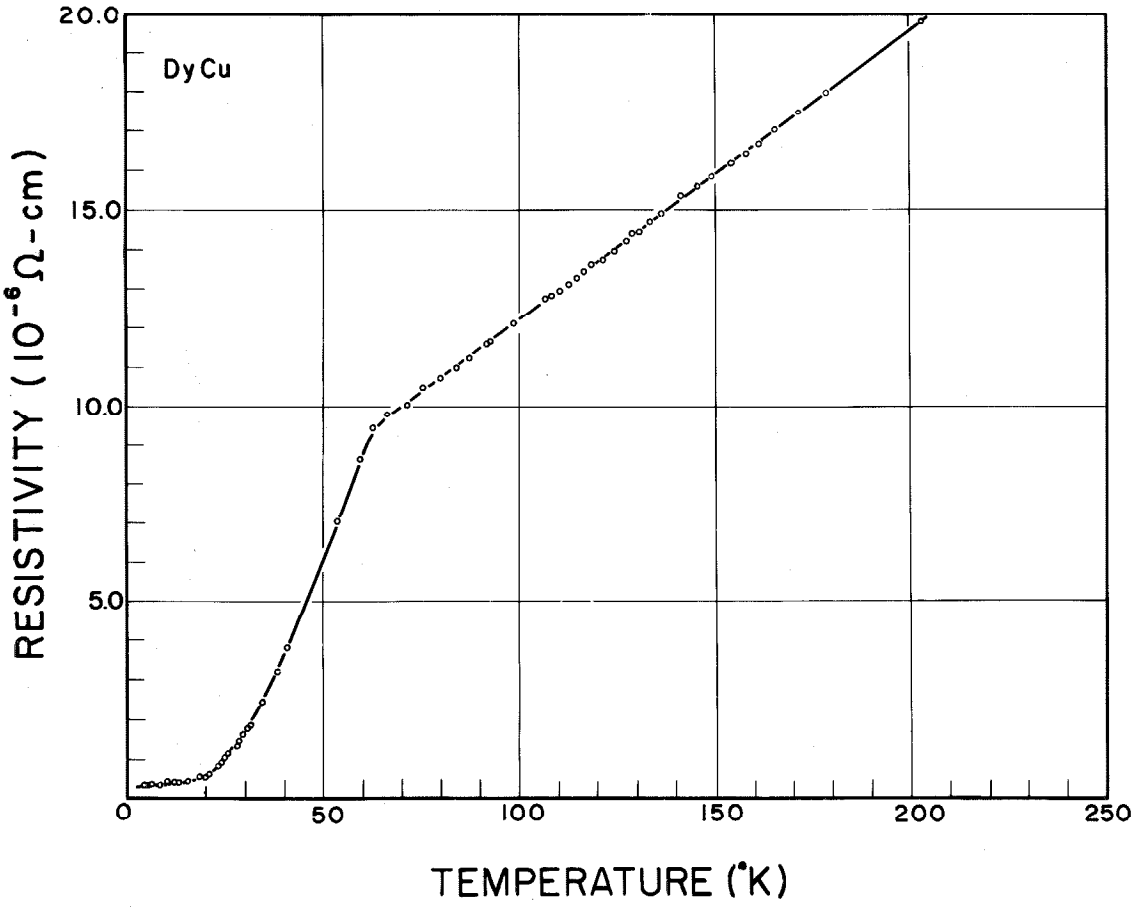

Fig. 10. Resistivity-Temperature Relationship for DyCu Intermediate Phase

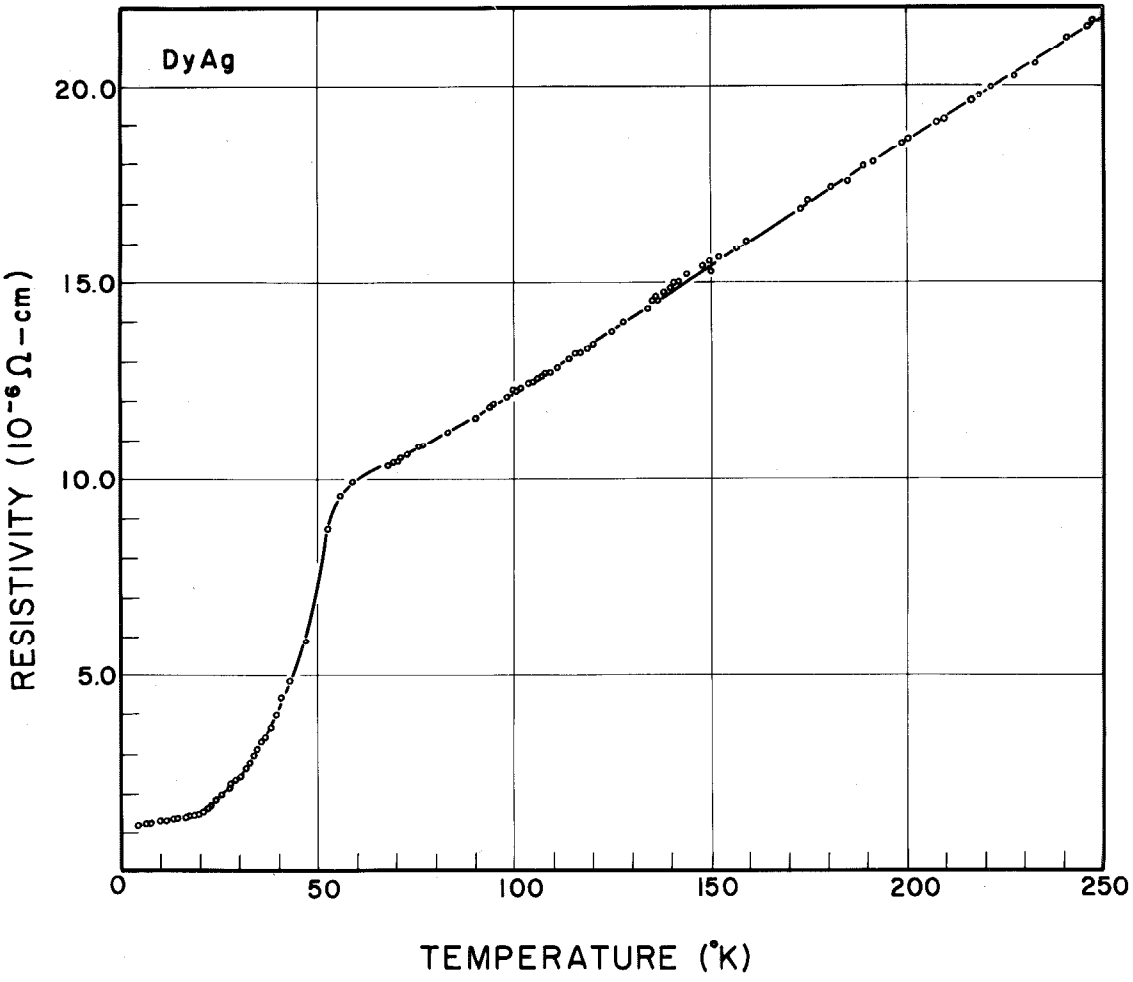

Fig. 11. Resistivity-Temperature Relationship for DyAg Intermediate Phase

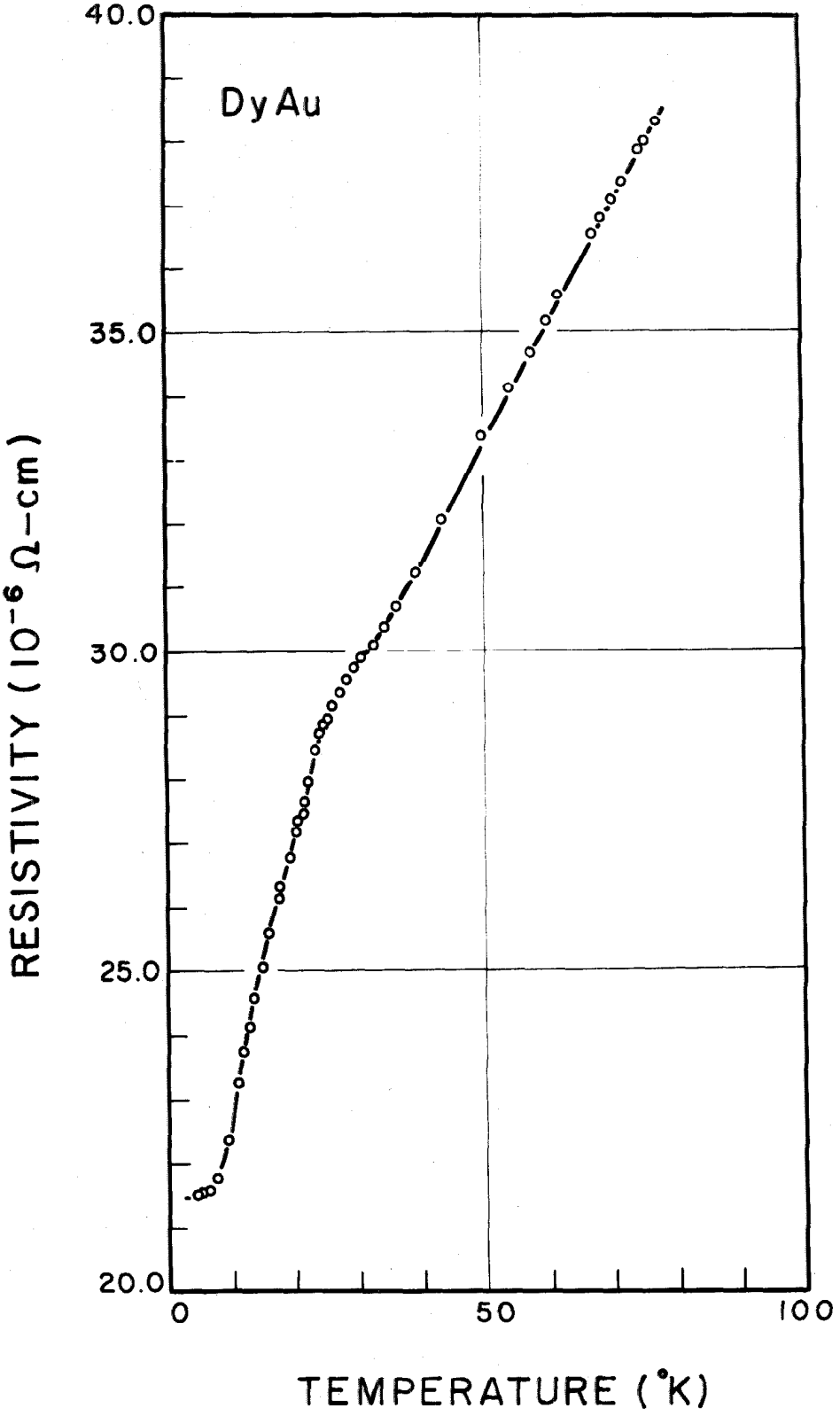

Fig. 12. Resistivity-Temperature Relationship for DyAu Intermediate Phase

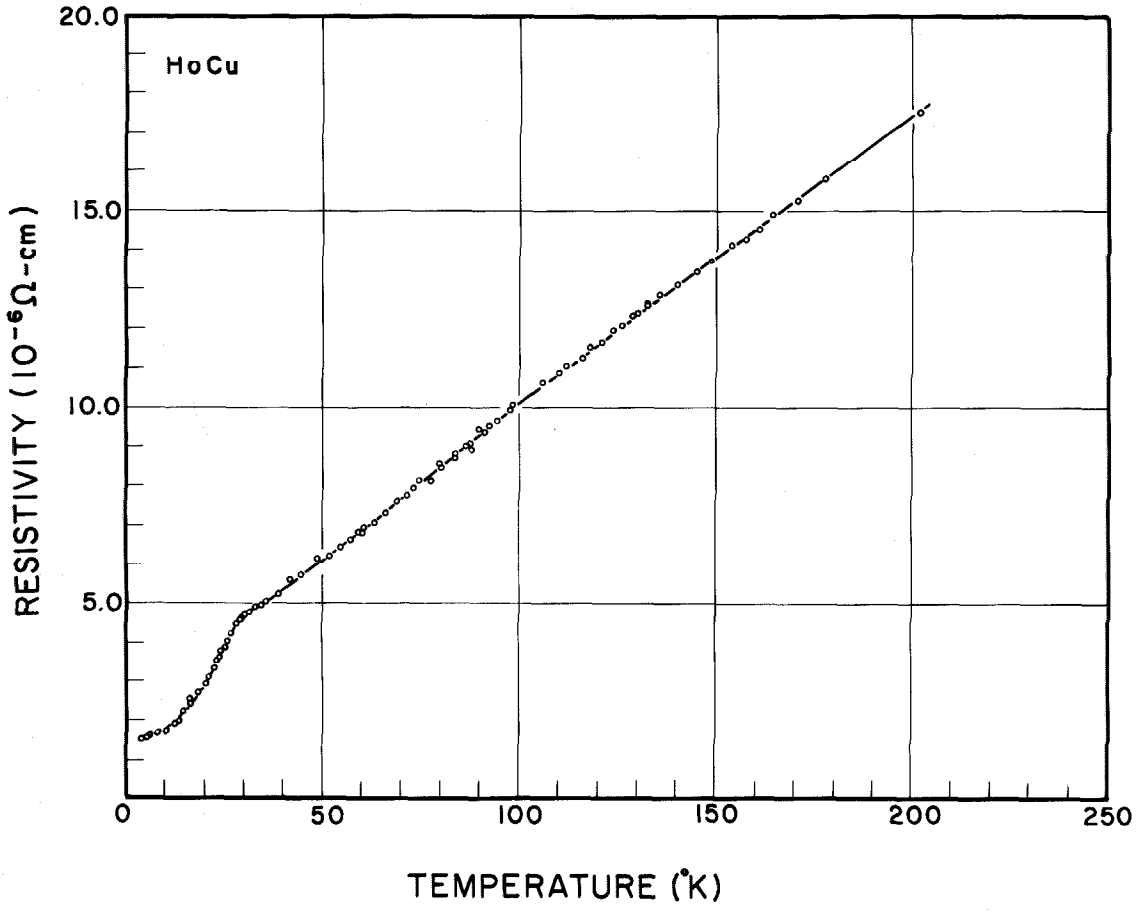

Fig. 13. Resistivity-Temperature Relationship for HoCu Intermediate Phase

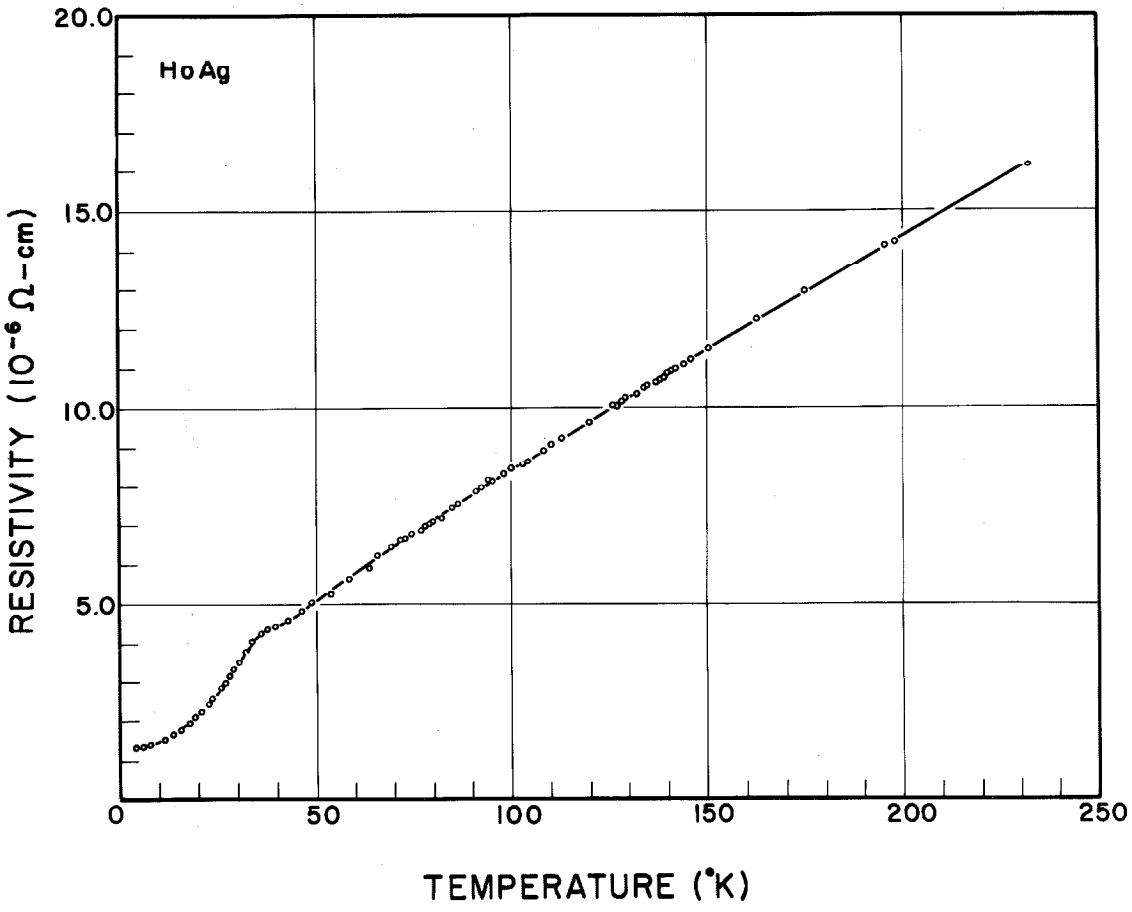

Fig. 14. Resistivity-Temperature Relationship for HoAg Intermediate Phase

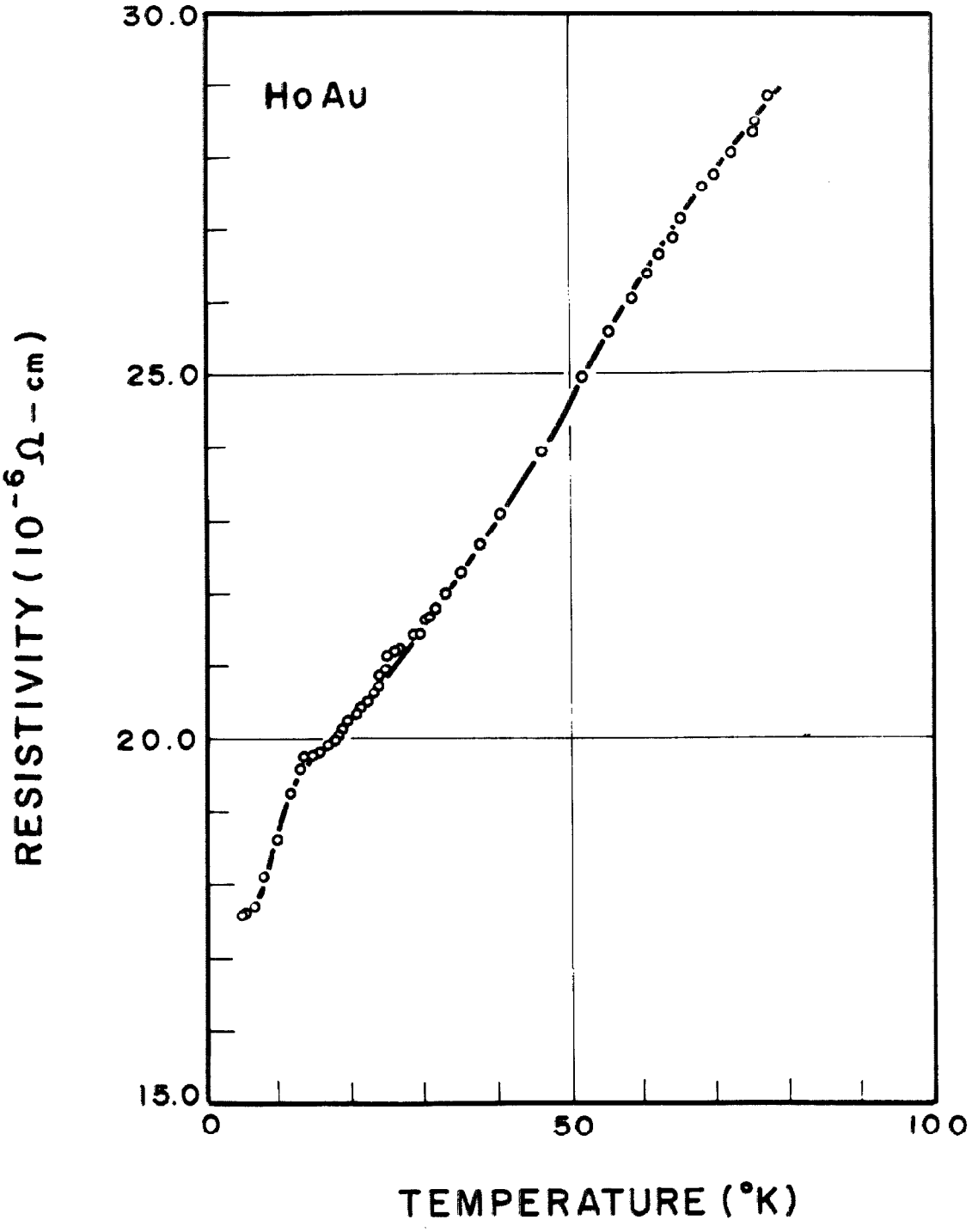

Fig. 15. Resistivity-Temperature Relationship for HoAu Intermediate Phase

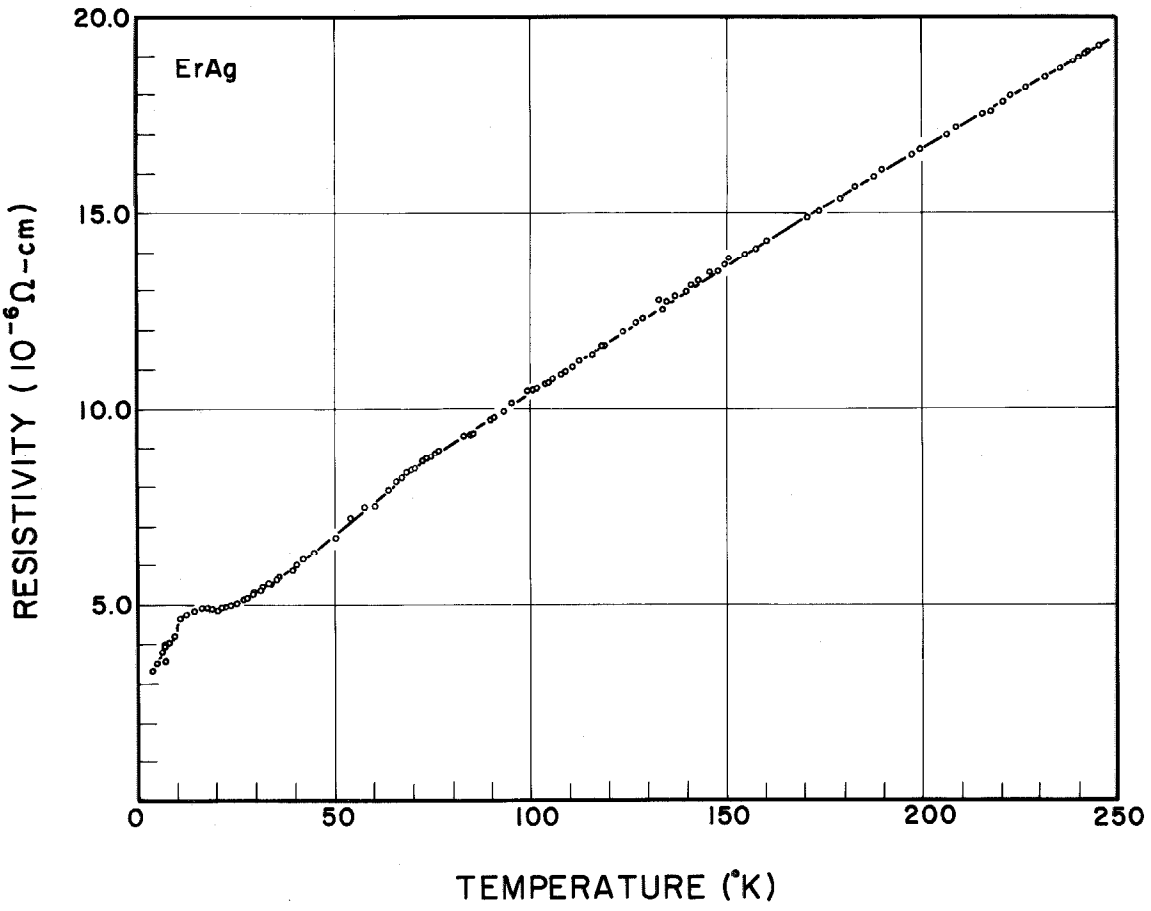

Fig. 16. Resistivity-Temperature Relationship for ErAg Intermediate Phase

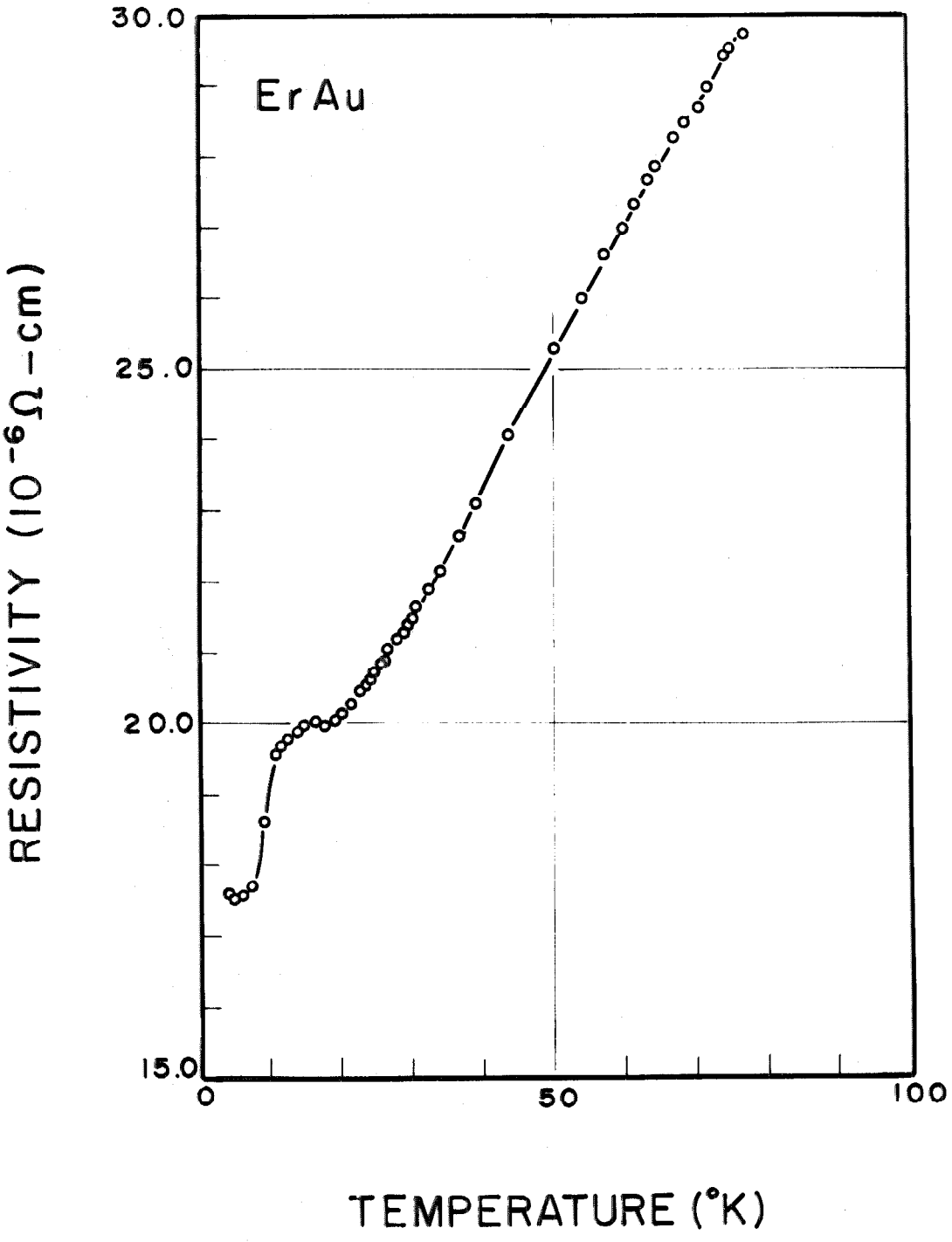

Fig. 17. Resistivity-Temperature Relationship for ErAu Intermediate Phase

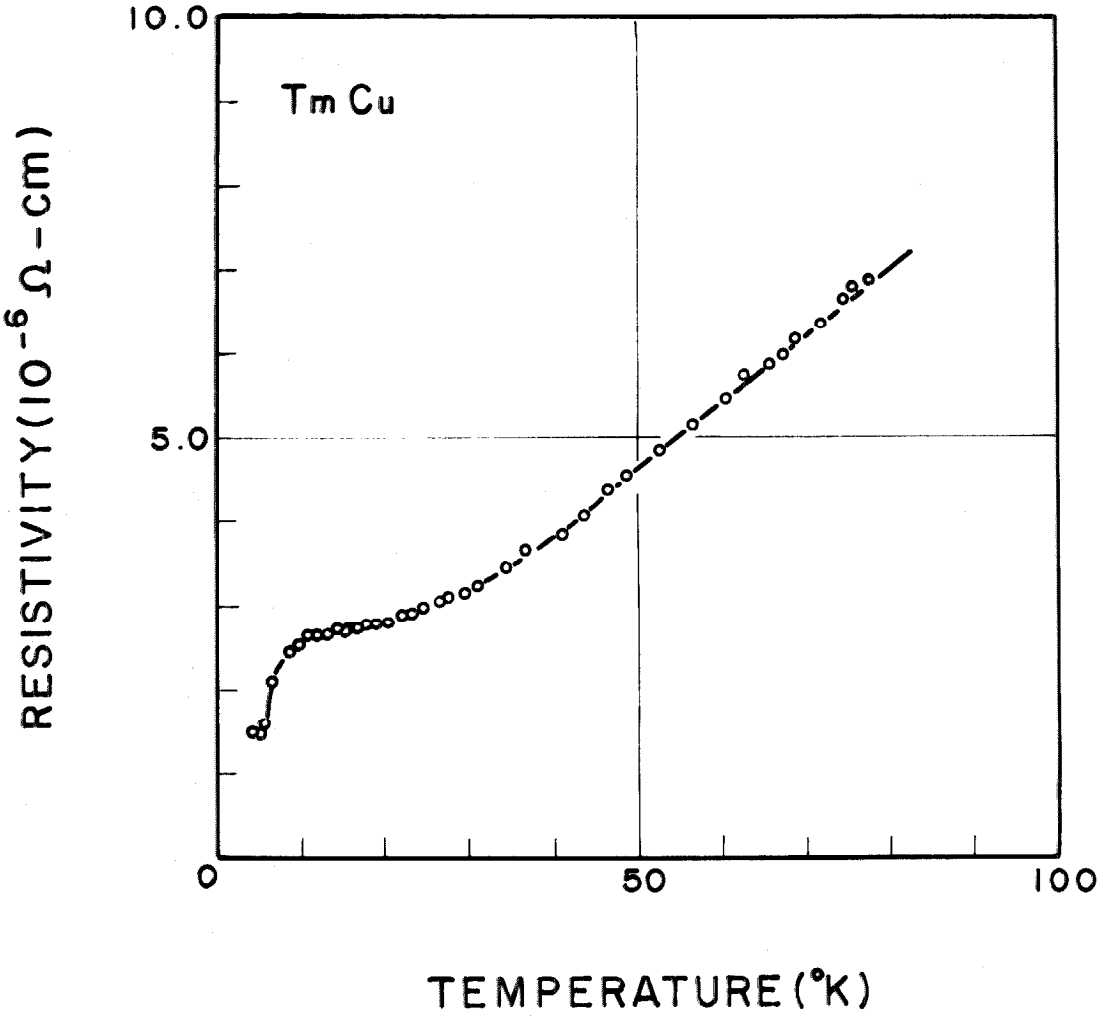

Fig. 18. Resistivity-Temperature Relationship for TmCu Intermediate Phase

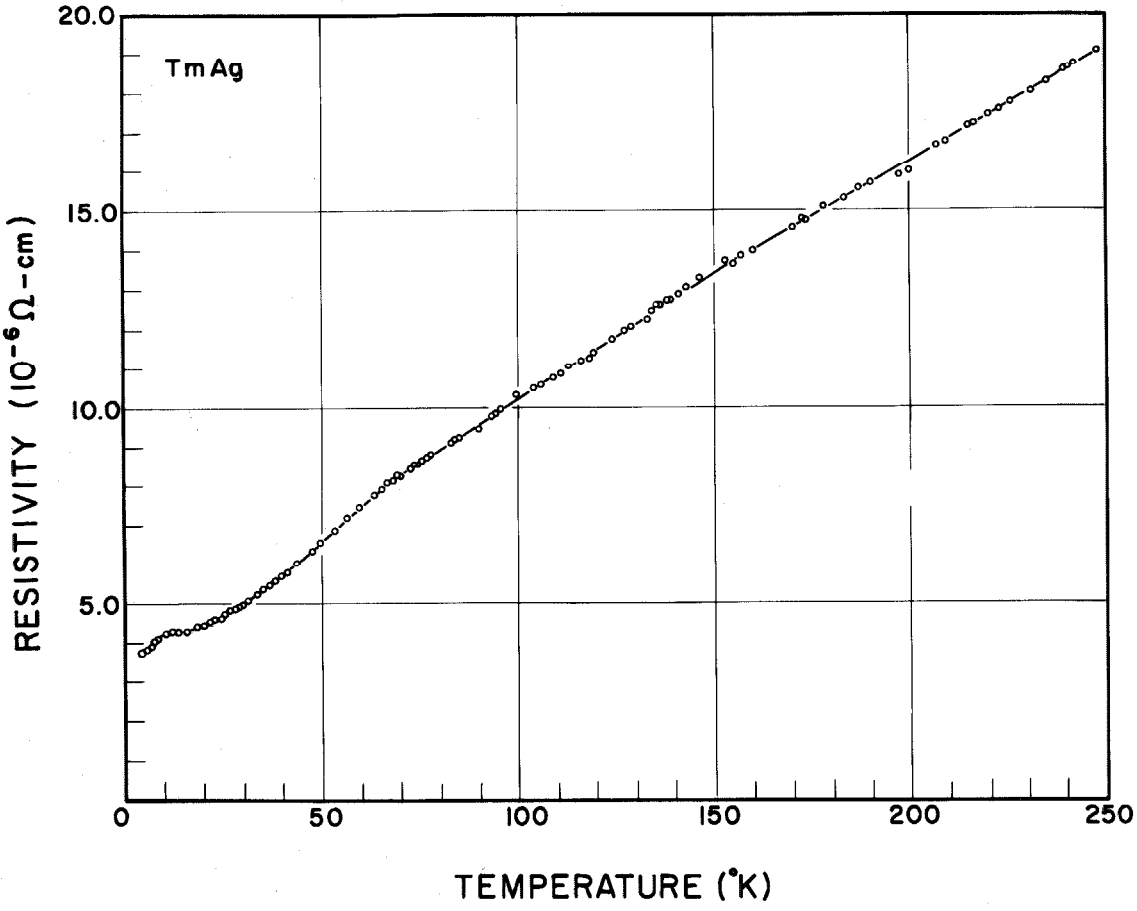

Fig. 19-1. Resistivity-Temperature Relationship for TmAg Intermediate Phase

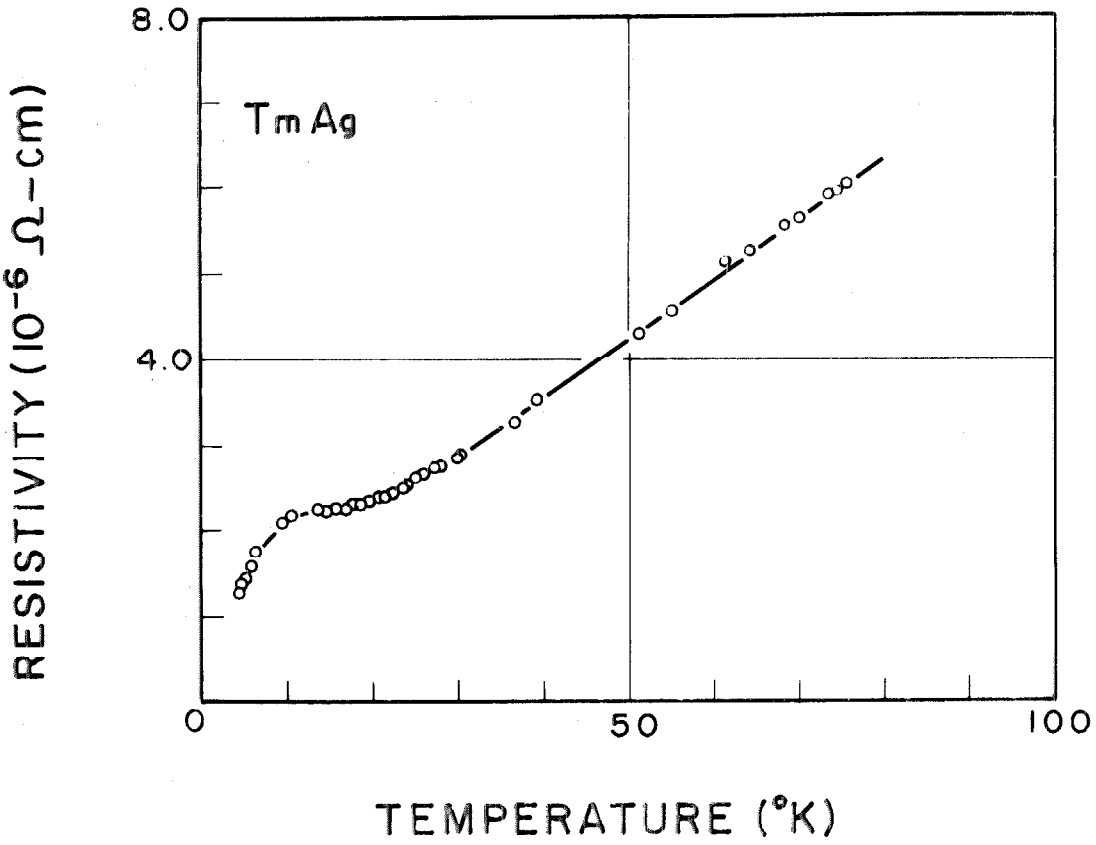

Fig. 19-2. Resistivity-Temperature Relationship for TmAg Intermediate Phase

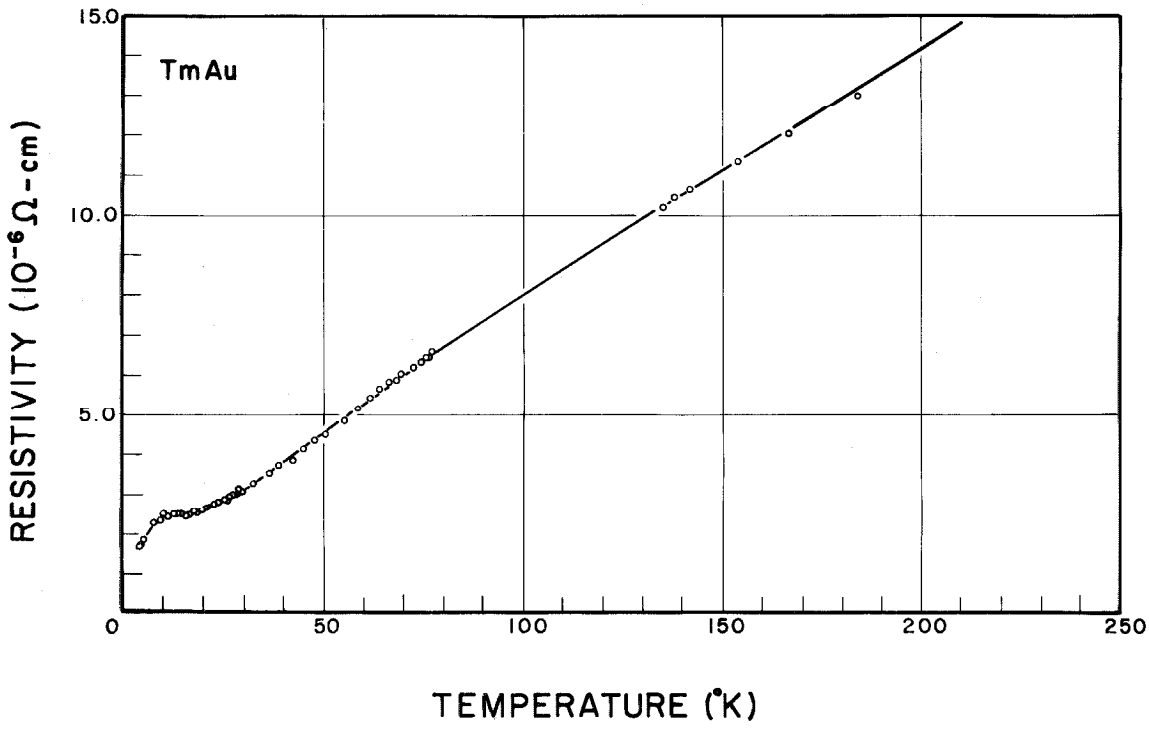

Fig. 20-1. Resistivity-Temperature Relationship for TmAu Intermediate Phase

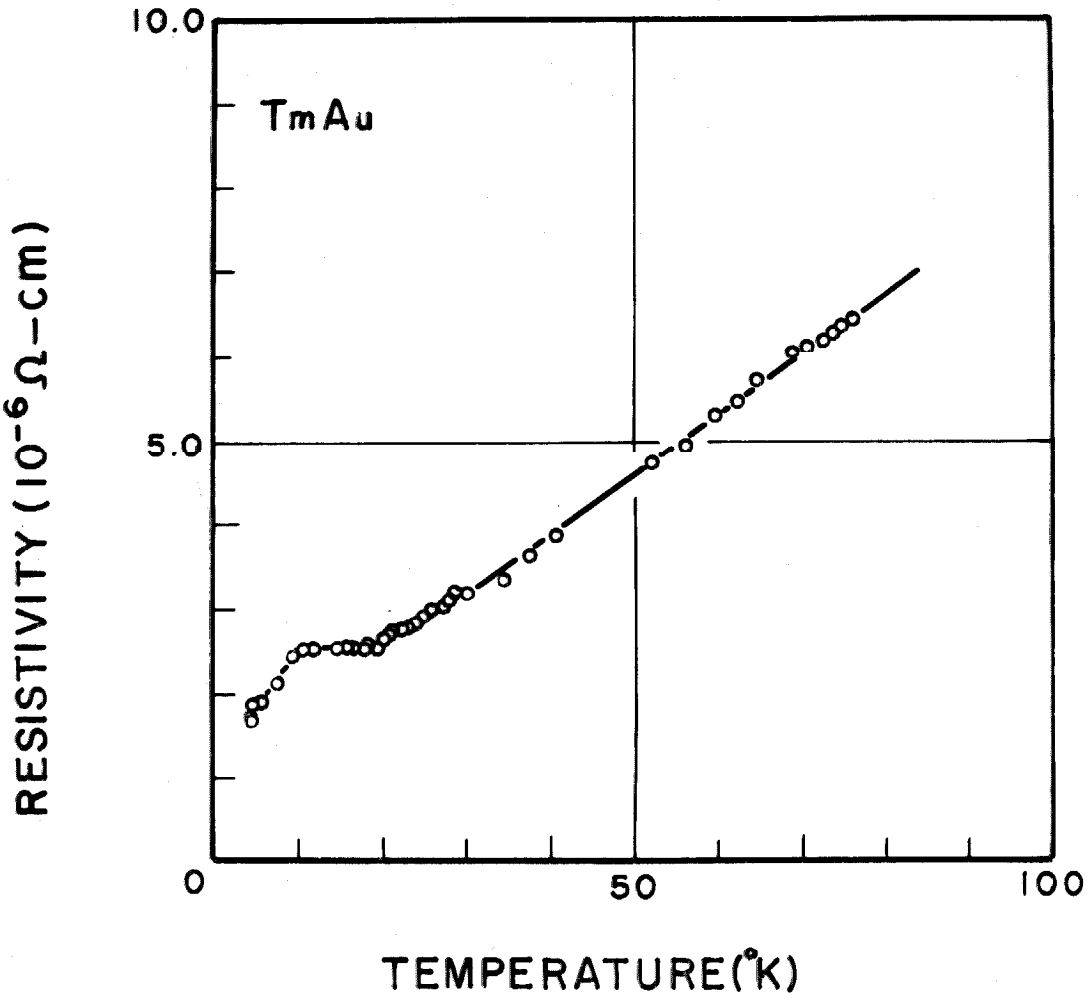

Fig. 20-2. Resistivity-Temperature Relationship for TmAu Intermediate Phase

C. DISCUSSION

The existence of an anomaly in the resistivity-temperature curves of the CsCl phases included in this investigation constitute an indirect evidence for a transition from a paramagnetic to an antiferromagnetic state. Previously reported results of neutron diffraction analysis of some of these phases established the existence of such transitions.[23] Six more CsCl phases were studied by Cable.[33] In addition, studies of magnetic susceptibility of some of the CsCl rare earth phases with Ag were carried out by R. Walline,[34] and paramagnetic to antiferromagnetic transitions were also found. All these results, together with those found in this investigation are compiled in TABLE 9. With the exception of the phases AgGd and AgTb, the agreement between the transition temperatures found by three different techniques (whenever possible) is relatively good considering the experimental difficulties inherent to each technique and also the fact that the relative amounts of impurities in the rare earth metals used for preparing the alloys may have been different by one order of magnitude.

For easier comparision, the curves of Figure 2 to 20 have been retraced in groups based on the composition of the alloys. The resistivity temperature curves of all CsCl phases containing Cu are presented in Figure 21. Those containing Ag and Au are given in Figures 22 and 23 respectively. And the curves for the CsCl phases containing a given rare earth and Cu, Ag, and Au have also been retraced in Figure 24 (Gd phases), 25 (Dy and Tb phases) and 26 (Tm, Er and Ho phases). These curves cover a wide range of

TABLE 9

Transition Temperature or Temperature Range of CsCl Phases

Phase	Transition Temperature or Range		
	This Investigation (^{o}K)	Neutron Diffraction (^{o}K)	Magnetic Susceptibility (^{o}K)
CuGd	135-145	---	---
CuTb	100-118	115	---
CuDy	62	62	---
CuHo	27	---	---
CuEr	---	33	---
CuTm	10-28	---	---
AgY	None	---	Pauli paramagnetic
AgNd	24-28	---	22
AgGd	137-140	---	118
AgTb	102-122	100	106
AgDy	53-65	64	55
AgHo	32-42	---	32
AgEr	10-24	34	15
AgTm	9-20	---	9.5
AuGd	42-50	---	---
AuTb	48-62	---	---
AuDy	24-34	---	---
AuHo	13-16	---	---
AuEr	13-19	---	---
AuTm	8-19	---	---

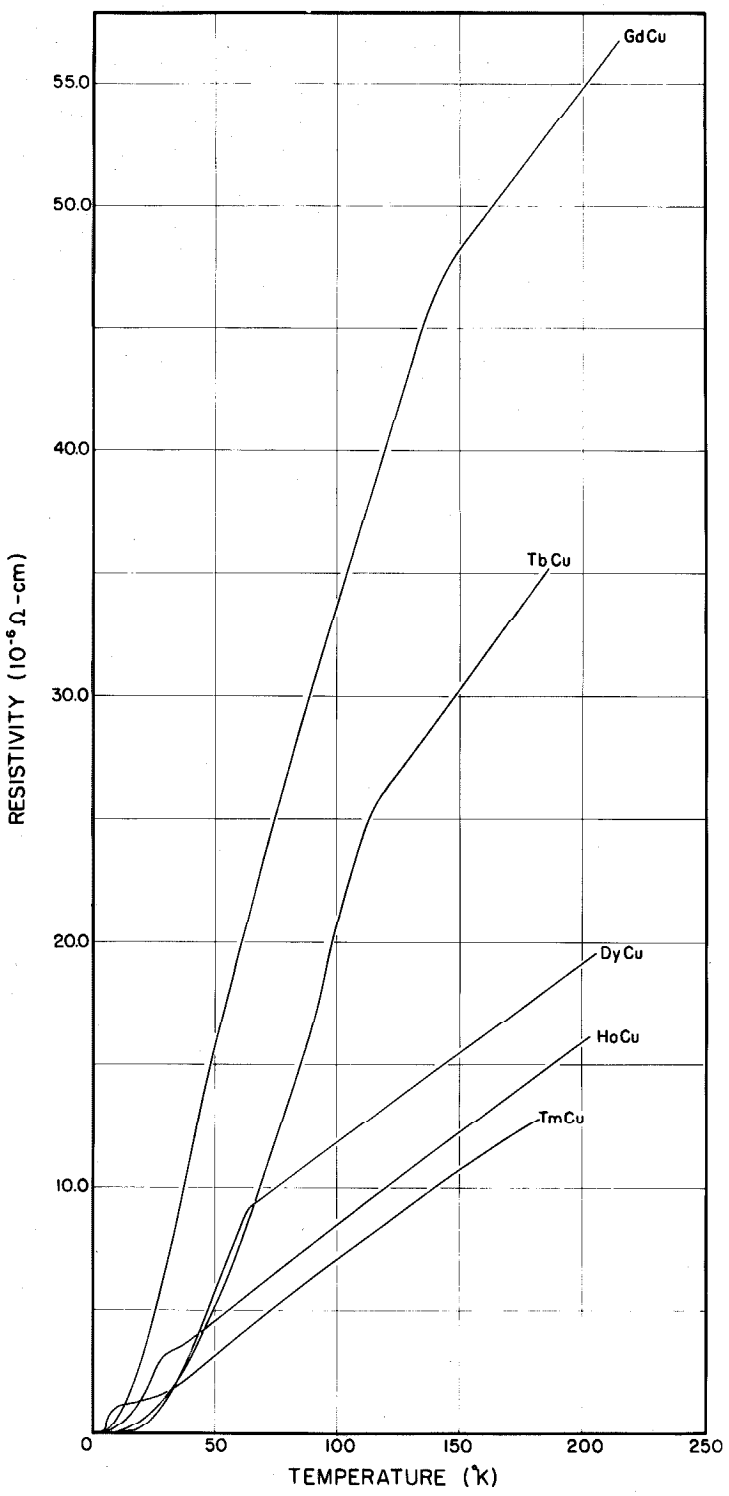

Fig. 21. Comparison of The Resistivity-Temperature Curves of the RCu Intermediate Phases

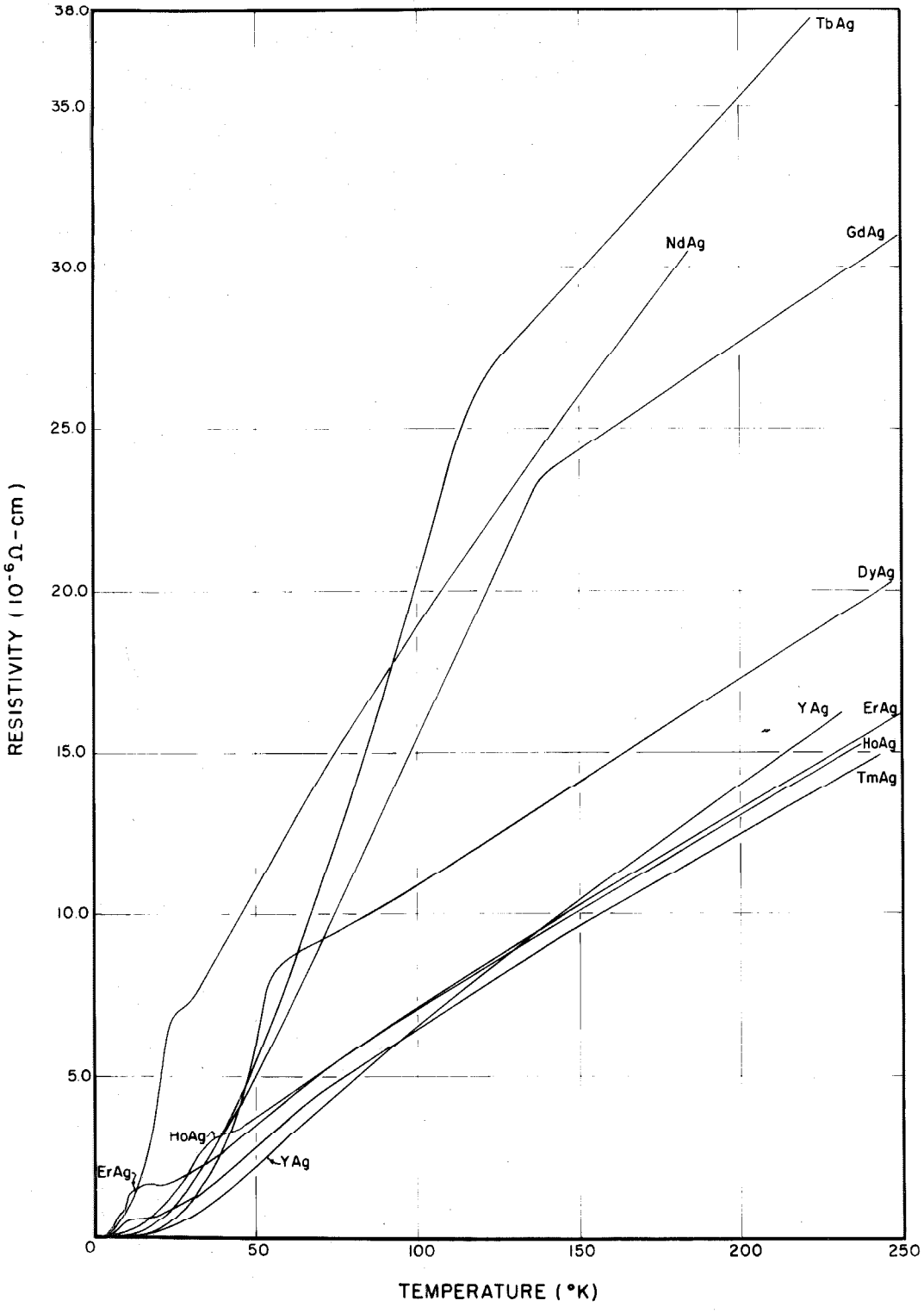

Fig. 22. Comparison of The Resistivity-Temperature Curves of The RAg Intermediate Phases

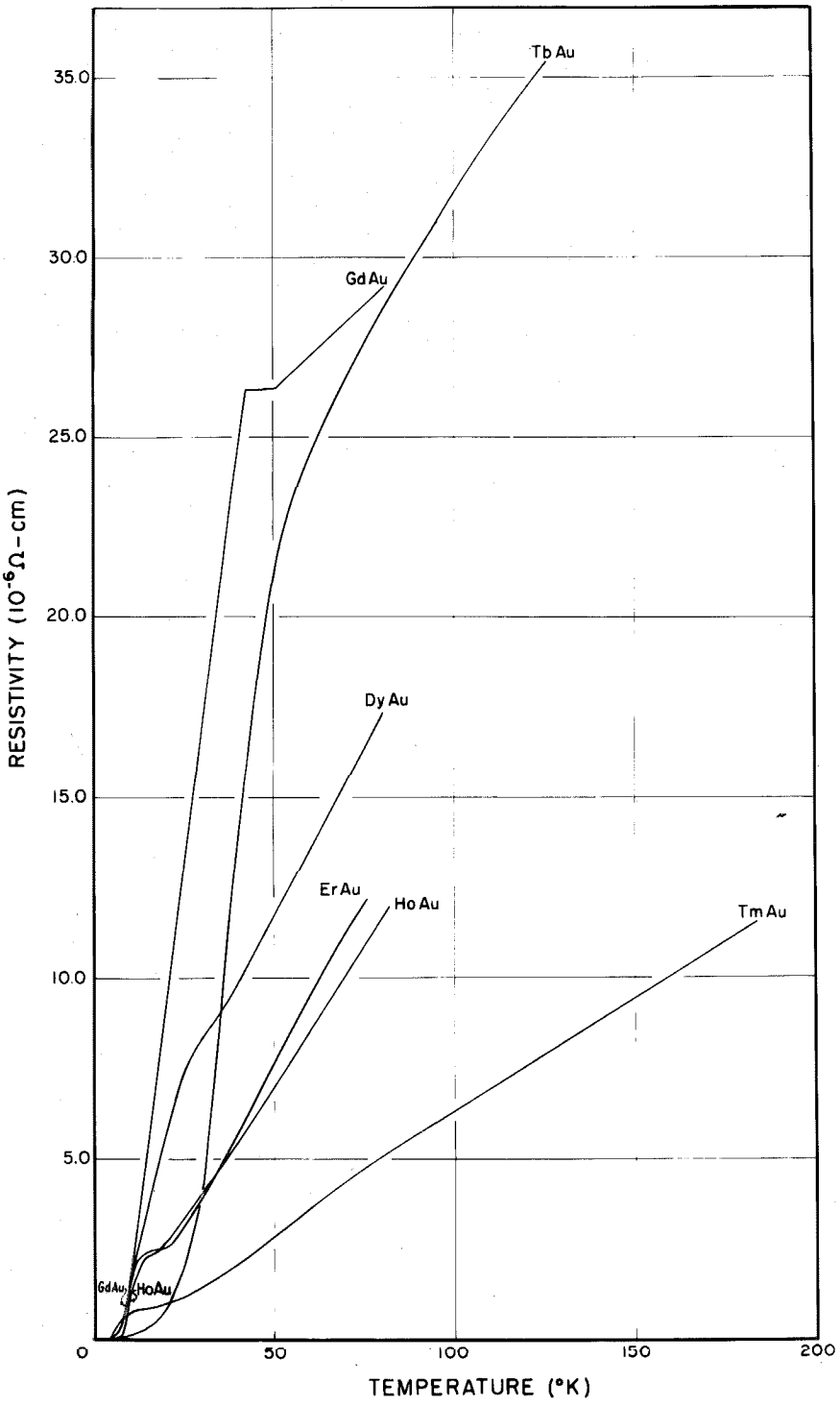

Fig. 23. Comparison of The Resistivity-Temperature Curves of The RAu Intermediate Phases

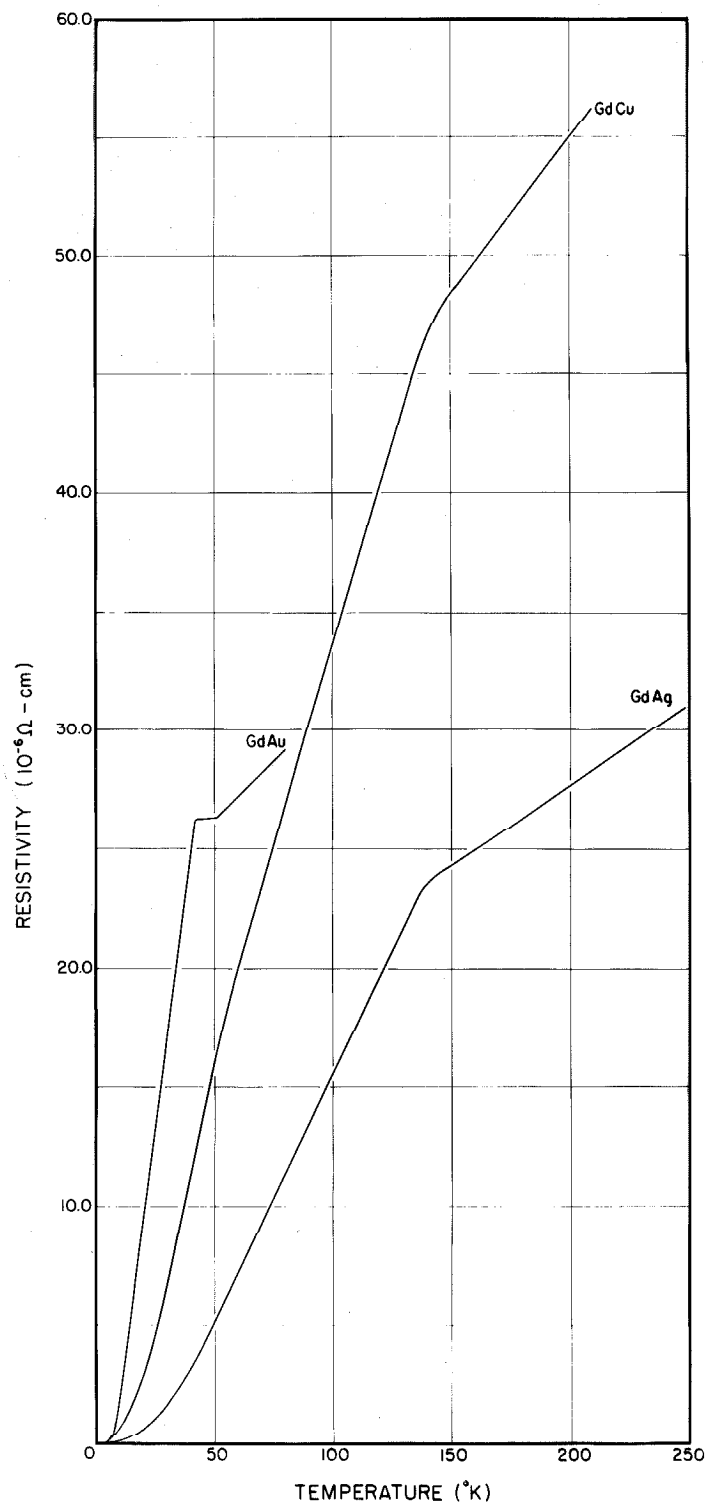

Fig. 24. Comparison of The Resistivity-Temperature Curves of The CsCl Phases of GdCu, Ag and Au

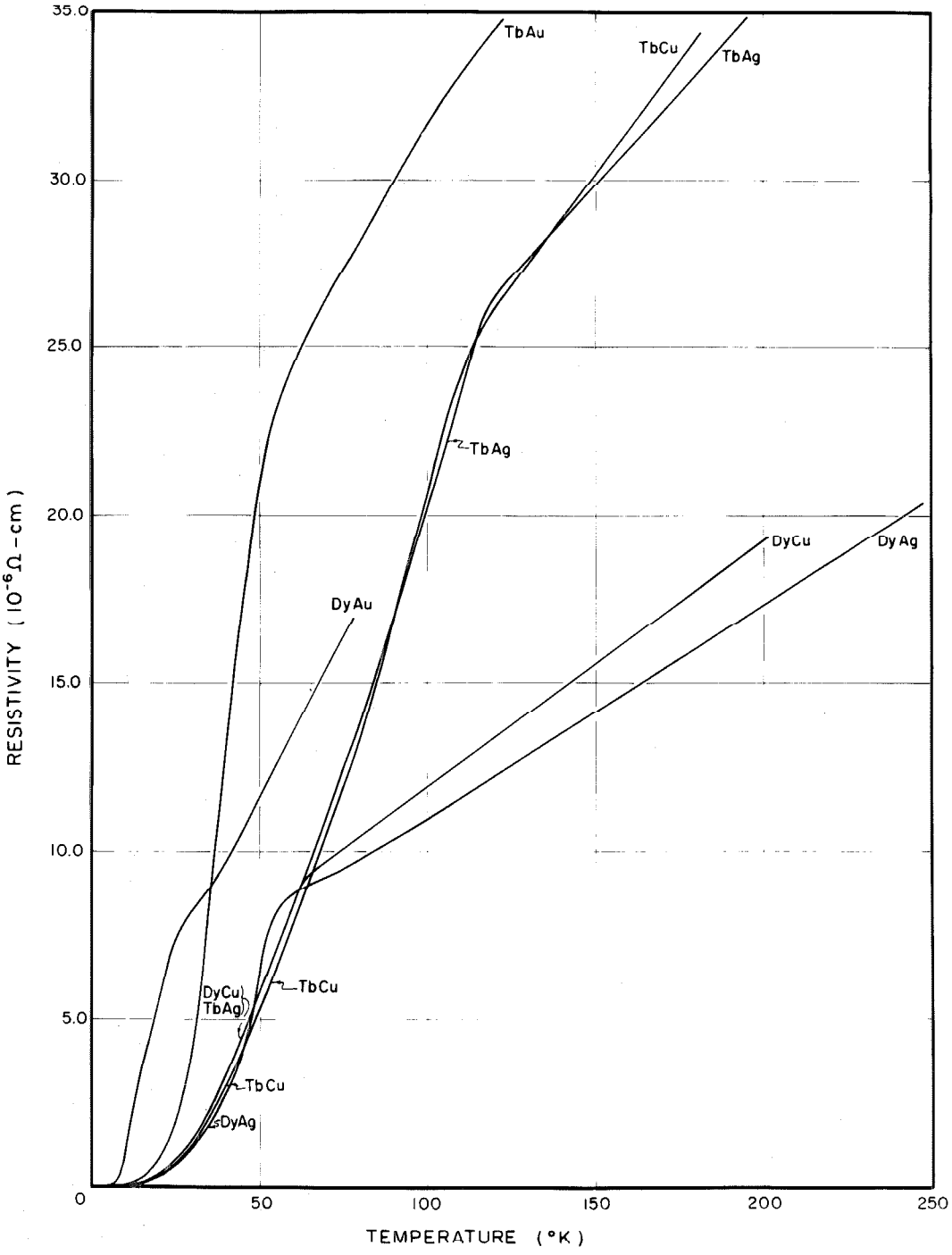

Fig. 25. Comparison of The Resistivity-Temperature Curves of The CsCl Phases of Tb, Dy and Cu, Ag, Au

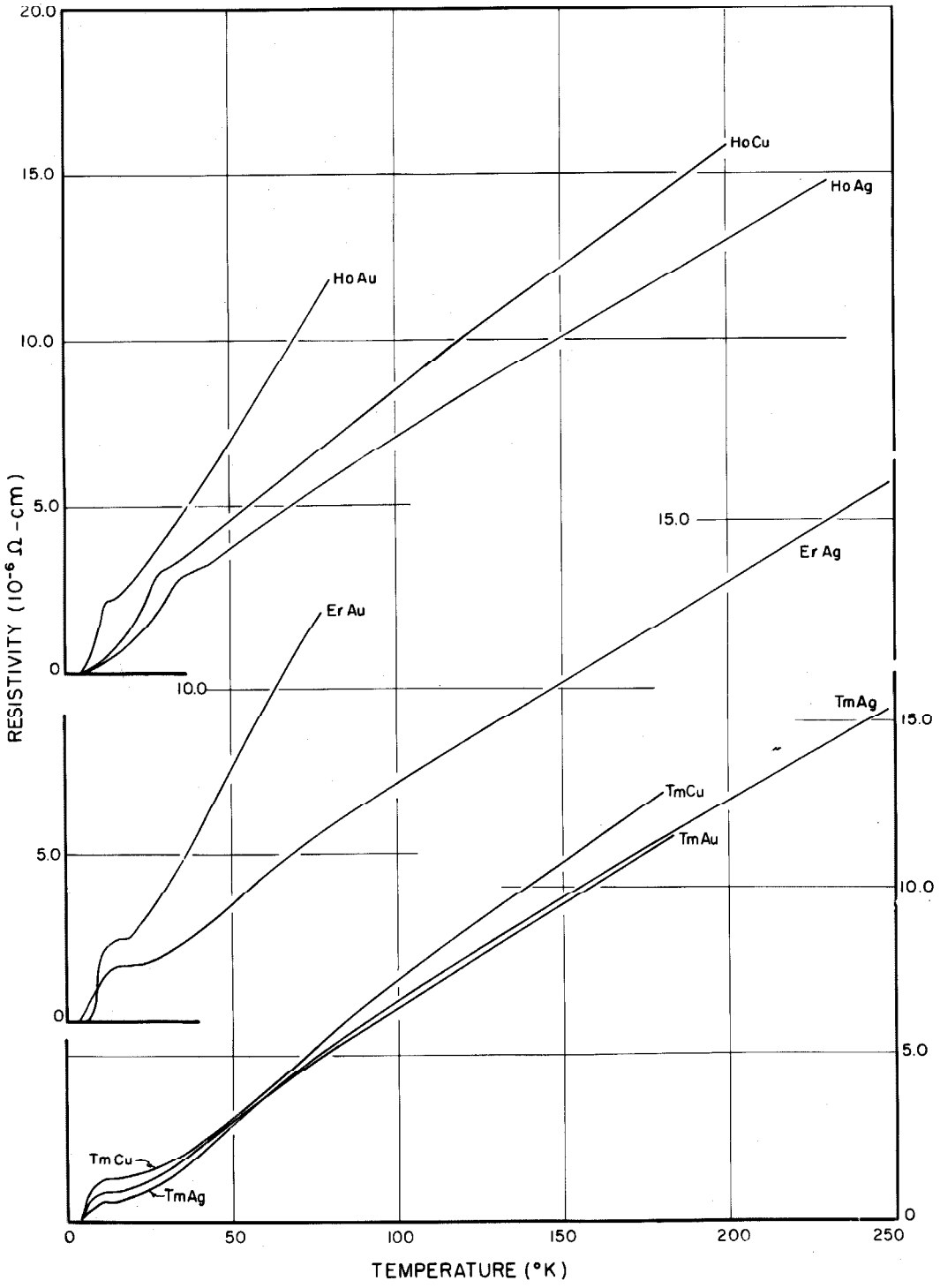

Fig. 26. Comparison of The Resistivity-Temperature Curves of The CsCl Phases of Ho, Er, and Tm with Cu, Ag, and Au

resistivity values and only very general statements can be made on the transition temperatures. With a few exceptions, it seems that the transition temperature, for a given phase containing a given metal (either Cu, Ag, or Au) decreases with increasing atomic number of the rare earth element, which corresponds to filling up of the 4f shells. There is also a general trend for the resistivity of the alloys at high temperature (10 to 150^{o}K) to decrease with increasing atomic number. According to the general expression for the resistivity at high temperatures, the values of the slope of the resistivity-temperature curves at high temperature would be all alike for metals of similar Debye temperatures and similar conduction electron configuration. Hence from the observation of the curves in Figures 21 to 26 and also from the fifth column of TABLE 10, at temperatures higher than the transition temperatures, we may guess that the conduction electron configuration and the Debye temperatures of the CsCl phases of DyCu, HoCu and TmCu are similar, those of GdAg, DyAg, ErAg, HoAg, TmAg and TmAu are similar and those of DyAu, ErAu and HoAu are similar. Also from Figure 22, we see that TbCu, TbAg, TbAu have more similarities to each other than to the CsCl phases of Cu, Ag and Au with other rare earth elements respectively.

The residual resistivities ρ_o listed in TABLE 10 are, in general, very low except those of gold alloys, and for GdCu and NdAg phases. These alloys probably contain more lattice imperfections than the other phases. In the fourth column of TABLE 10, the slopes of only four of the resistivity-temperature

curves below the transition temperature are given, for the others no definite value can be given because the changes of resistivity vs. temperature are not linear. The slopes for temperatures above transition temperature are given in the fifth column. In the last column of TABLE 10, a transition type according to the resistivity-temperature curves is specified. Type I is a transition in which the slope of ρ - T curve has no extremum around the transition temperature and Type II is a transition in which the slope of ρ - T curve has one or more extremum. The existence of such differences also existed in the ρ - T curve for pure rare earth elements, but no explanation is apparent at this moment.

TABLE 10

Summary of Results on

The Resistivity-Temperature Curves of CsCl Phases

CsCl Phase	ρ_r ($\mu\Omega$-cm)	Transition Range (^oK)	$(\partial\rho/\partial T)^b$ $\mu\Omega$-cm/ ^oK	$(\partial\rho/\partial T)^a$ $\mu\Omega$-cm/^oK	Transition Type†
YAg	3.7	none	--	--	--
NdAg	7.8	24-28	0.5	0.15	II
GdCu	15.0	135-145	0.33	0.15	I
GdAg	2.6	137-140	0.22	0.07	I
GdAu	28.5	42-50	0.8	0.09	II
TbCu	3.4	100-118	--	0.14	I
TbAg	5.3	102-122	--	0.11	I
TbAu	23.3	48-62	--	--	I
DyCu	0.35	62	--	0.07	II
DyAg	1.2	53-65	--	0.06	II
DyAu	21.5	24-34	--	0.18	II
HoCu	1.6	27	--	0.08	II
HoAg	1.3	32-42	--	0.14	II
HoAu	17.5	13-16	--	0.15	II
ErAg	3.3	10-24	--	0.06	II
ErAu	17.5	13-19	--	0.17	II
TmCu	1.5	10-28	--	0.07	II
TmAg	1.3	9-20	--	0.07	II
	3.7	9-20	--	0.07	II
TmAu	1.7	8-19	--	0.06	II

$(\partial\rho/\partial T)^b$: Slope of the $\rho(T)$ curve below transition temperature.

$(\partial\rho/\partial T)^a$: Slope of the $\rho(T)$ curve above transition temperature.

† : Type I is a transition in which the slope of the resistivity-temperature curve decreases more or less sharply from the low temperature value to the higher temperature value. Type II is a transition in which the slope of the resistivity-temperature curve decreases to a value equal or nearly equal to zero and then increases to high temperature value.

V. THEORETICAL CONSIDERATION ON THE RESISTIVITY - TEMPERATURE RELATIONSHIP IN CSCL PHASES CONTAINING RARE EARTH ELEMENTS

The electrical conductivity of metallic elements has long been a most difficult subject in theoretical physics. The most general expression for the electrical resistivity is based on the Boltzmann's equation

$$-\vec{v}_k \cdot \frac{\partial f}{\partial \vec{r}} - \frac{e}{\hbar}\left(\vec{E} - \frac{1}{c}\vec{v}_k \times \vec{H}\right) \cdot \frac{\partial f}{\partial \vec{k}} = -\dot{f}_k \Big]_{scatt}$$

in which $\vec{E}$ is the electrical field vector, $\vec{H}$ the magnetic field vector, $\vec{v}_k$ is the velocity vector of electrons with wave vector $\vec{k}$, and e is the electron charge and $\hbar$ is the Plank constant divided by 2π. If the distribution function f_k could be obtained from this equation, then the electrical current density per unit volume can be calculated as

$$\vec{J} = \int e\, \vec{v}_k\, f_k \, d\vec{k}.$$

The linearized Boltzmann equation is of the form

$$-\vec{v}_k \cdot \frac{\partial f_k^o}{\partial T} \nabla T - \vec{v}_k \cdot e \frac{\partial f_k^o}{\partial \epsilon_k} \vec{E} = \int [(f_k - f_k^o) - (f_{k'} - f_{k'}^o)] Q_k^{k'} d\vec{k}'$$

where $Q_k^{k'}$ is the transition probability for electrons with wave vector k to k', and the elementary solution of this linearized equation is

$$f_k - f_k^o = -\vec{v}_k \cdot \left(\frac{\partial f_k^o}{\partial T} \nabla T - e \frac{\partial f_k^o}{\partial \epsilon_k} \vec{E}\right) \left[\int (1 - \cos\varphi) Q(k, \varphi)\, d\Omega\right]^{-1}$$

expressing the integral $\int (1-\cos\varphi)\, Q(k, \varphi)\, d\Omega$ by $1/\tau(k)$ then the resistivity is expressed as

$$\rho = \frac{4\hbar\pi^3}{e^2 \tau(R)} \left(\int \vec{v} \cdot d\vec{S} \right)^{-1}$$

where R is the Fermi radius, $\vec{v}$ the electron velocity and $d\vec{S}$ the elements of the Fermi surface.

The above results are obtained under the conditions: that the energy surfaces in k-space are spherical and that the scattering probability depends only on the angle between $\vec{k}$ and $\vec{k'}$ and not on their orientation in the crystal. From the above expressions, if the cross section per unit solid angle for scattering of a conduction electron by a scatterer is $\sigma(\varphi)$, then the total cross section

$$\sigma = 2\pi \int \sigma(\varphi) (1-\cos\varphi) \sin\varphi \, d\varphi$$

and the associated relaxation time is

$$\tau_i = \Lambda / v_f = n_i \sigma v_f$$

where v_f is the velocity at the Fermi energy, n_i the concentration of the scatterers, and Λ the mean free path. The resistivity due to these scatterers then has the form

$$\rho_i = m^*/ne^2\tau_i = (n_i k_f/ne^2)\sigma$$

for a spherical Fermi surface. It is in τ_i that all the interaction mechanisms and the crystal structure or the Fermi surfaces of a given metal or alloy have been taken into consideration.

In general the contribution to the resistivity of a given element or alloy are from several different sources. They can be either separated or not separated from each other. For pure rare earth elements, the resistivity can be considered as formed mainly from three parts: i) phonon scattering of the conduction electrons, ρ_{ph}; ii) spin disordering scattering, ρ_s; iii) residual resistivity ρ_r due to lattice imperfections and impurities.

Usually, ρ_r is independent of temperature, and ρ_{ph} in general varies linearly with temperature at high temperatures. The part ρ_s due to the scattering of conduction electrons by spin disordering can be considered as constant at temperatures higher than the transition temperature. Thus if the $\rho(T)$ curve is extrapolated from the high temperature linear part down to zero temperature and the residual resistivity subtracted, the spin disordering component ρ_s can be obtained. This has been done for pure rare earth elements (28), (29), (30), (35). The ρ_s part for rare earth elements has been studied by several authors, and the important parts are briefly summarized in the following paragraphs.

It has been recognized by de Gennes and Friedel[36),(37)] that the localized 4f electrons played an important role in the anomalous magnetic and electrical properties of pure rare earth elements. The localized 4f electrons at each ion in the metal are interacting with their neighboring magnetic ions through their polarization of the conduction electrons. If $\vec{s}_e(\vec{r})$ represents the spin of the conduction electrons at $\vec{r}$ and $\vec{S}_{f_i}$ the spin of the i-th 4f electron of a given ion, then according to de Gennes' model, the exchange interaction of the

conduction electron with 4f electrons at a given ion is

$$-\Gamma \sum_i \vec{s}_e \cdot \vec{S}_{f_i}$$

where Γ is the coupling constant, which is almost a constant through the series of rare earth elements. If the influence on the energy level of this interaction is small, $\sum_i \vec{S}_{f_i}$ can be replaced by $(g-1)\vec{J}$, where g is the Lande factor of the ion. Then the interaction is expressed as

$$-\Gamma (g-1) \vec{s}_e \cdot \vec{J}$$

and the ionic angular moment $\vec{J}$ polarizes the spin $\vec{s}_e(\vec{r})$ of the conduction electron at $\vec{r}$. According to Kittel[38], Yoshida[39] and Rocher[35], if the Fermi surface of the rare earth elements is approximated as spherical, the polarized spin density $\vec{s}_e(\vec{r})$ is given by

$$\vec{s}_e(\vec{r}) = -\frac{9\pi}{4} Z^2 \frac{\Gamma(g-1)}{V^2 E_f} F(2k_f r) \vec{J}$$

where Z is the ionic charge, V is the atomic volume, E_f is the Fermi energy and $\vec{k}_f$ the corresponding wave vector. $F(\xi)$ is the Ruderman-Kittel function:

$$F(\xi) = \frac{\xi \cos\xi - \sin\xi}{\xi^4}$$

Because of the polarization of the conduction electrons by the ion, an indirect interaction between ions at $\vec{R}_m$ and $\vec{R}_n$ which are $\vec{R}_{mn}$ apart is produced in the following manner:

$$I_{mn} = \frac{9\pi}{4} Z^2 \frac{\Gamma^2 (g-1)^2}{V^2 E_f} F(2k_f R_{mn}) \vec{J}_m \cdot \vec{J}_n$$

$\vec{J}_m$, $\vec{J}_n$ are the angular momentum of the ions m, and n respectively[35], [37]. Then the total energy due to the indirect exchange mechnism by means of conduction electrons is

$$E = \sum_{m \neq n} I_{mn}$$

which depends on both the temperature and the crystal structure of a given element.

The magnetic susceptibility in the paramagnetic region given by the interaction I_{mn} is of the form of $C/(T-\theta_p)$, with θ_p given by

$$k_B \theta_p = - \frac{3\pi}{4} Z^2 \frac{\Gamma^2 (g-1)}{V^2 E_f} j(j+1) \sum_{n \neq o} F(2k_f R_{on})$$

where R_{on} is the distance between the ion site o and another ion site n in the lattice. The electrical resistivity due to the disordering of the spins of the ions in the paramagnetic region of the elements is

$$\rho_s = \frac{3\pi}{8} \frac{m^*}{he^2} \Gamma^2 \frac{(g-1)^2}{V E_f} j(j+1)$$

with m^* being the effective mass of the conduction electrons. The calculations done by Rocher, for the given ρ_s and θ_p for Gd indicated that $\Gamma = 5.7$ ev-$\mathring{A}^3$, and $m^* = 3$. By assuming that these values of Γ and m^* are constant throughout the rare earth elements, a very good agreement with the experimental values was reached for

the values of ρ_s and θ_p for rare earth elements other than Gd.

However, Kasuya[40] approached the problem in a detailed way. The basic Hamiltonian he used is of the form of

$$\mathcal{H} = \sum_i \frac{p_i^2}{2m} + \sum_n \sum_i v_o(|\vec{r} - \vec{R}_n|) + \sum_{i>j} \sum_j e^2/r_{ij}$$

where the first term is the kinetic energy of the electrons, the second term the interaction between the electrons and the ions, and the third term the coulomb interaction between electrons. Using the second quantization technique and assuming the Bloch type wave function for conduction electrons and atomic wave function for the unfilled shell electrons, he obtained the above Hamiltonian in the following form:

$$\mathcal{H} = \sum_k \sum_\nu E_k a^\dagger_{k\nu} a_{k\nu} - N^{-1} \sum_k \sum_{k'} \sum_n J(\vec{k} - \vec{k}') e^{i(\vec{k}-\vec{k}')\cdot\vec{R}_n}$$
$$[(a^\dagger_{k+} a_{k'+} - a^\dagger_{k-} a_{k'-}) S^z_n + a^\dagger_{k+} a_{k'-} S^-_n - a^\dagger_{k'-} a_{k+} S^+_n]$$

where $a^\dagger_{k\nu}$, $a_{k\nu}$ are the creation and destruction operators for conduction electrons of wave vector $\vec{k}$ and spin ν; S^z_n, S^+_n, S^-_n are the spin operators of the magnetic ions; and N is the number of the magnetic ions in a unit volume;

$$J(\vec{k}-\vec{k}') = N \iint d\vec{r}_1\, d\vec{r}_2\, \varphi^*_{dn}(\vec{r}_1)\, \varphi^*_k(\vec{r}_2) \frac{e^2}{r_{12}} \varphi_{dn}(\vec{r}_2) \varphi_{k'}(\vec{r}_1) e^{i(\vec{k}'-\vec{k})\cdot\vec{R}_n};$$

and $\vec{k}$ is the wave vector of the conduction electrons under the assumption that conduction electrons behave like free electrons. By introducting the spin-wave operators,

$$\vec{S}_q = N^{-\frac{1}{2}} \Sigma_n \vec{S}_n e^{i \vec{q}\cdot\vec{R}_n}$$

$$\vec{s}_q = N^{-\frac{1}{2}} \Sigma_i \vec{s}_i e^{i \vec{q}\cdot\vec{r}_i}$$

and remembering the relation between the operators $a_k^\dagger$, a_k and the spins of electrons s_i of Holstein-Primakoff transformation, the Hamiltonian takes the following form,

$$\mathcal{H} = \sum_k \sum_\nu E_k a_{k\nu}^\dagger a_{k\nu} - \sum_q J(\vec{q})\, \vec{S}_q \cdot \vec{s}_{-q}$$

or

$$\mathcal{H} = \sum \frac{p_i^2}{2m} - \sum_i \sum_n J(|\vec{r}_i - \vec{R}_n|)\, \vec{S}_n \cdot \vec{s}_i$$

where

$$J(|\vec{r} - \vec{R}_n|) = N^{-1} \sum_q J(\vec{q})\, e^{i(\vec{r}_i - \vec{R}_n)\cdot\vec{q}}$$

and

$$\vec{q} = \vec{k} - \vec{k}' \,.$$

It is obvious that the second term is similar to that proposed by de Gennes. However this treatment by Kasuya is limited by the condition that the orbital angular momentum of the elements are quenched, and is applicable only to Gd in the rare earth series. Accepting the above interaction mechanism and assuming that the molecular field approximation is valid, the equation of the balancing of the total wave vector K under the assumptions of Kramer's

distribution function[41] $n_k = \left[\exp\left[(E_{\vec{k}} - E_f)/k_B T - \vec{c}\vec{k} \right] - 1 \right]^{-1}$, can be solved and the spin dependent part of the resistivity has the following form:

$$\rho_s = \frac{3\pi m^*}{Ne^2\hbar^2 E_f} (S - \sigma)(S + \sigma + 1) J_{eff}^2$$

where m^*: the effective mass of conduction electrons, N: the number of magnetic ions in an unit volume, $J_{eff}^2 = 4\int_0^1 J^2(2k_f x)\, x^3\, dx$, k_f: the wave vector of Fermi surface, and E_f: the Fermi energy, S: the spin quantum number of the ions, σ: the average orientation of S_n^z with $\sigma = S$ at $T = 0^\circ K$, and $\sigma = 0$ as $T > T_c$.

An improvement of the de Gennes and Friedel theory has been proposed by R. J. Elliott and F. A. Wedgwood[42]. They assumed the following model in trying to explain the electrical resistivity of single crystals of rare earth elements.

The ground state of the trivalent ion is described having a total angular moment $\vec{J}$ and a spin angular momentum $\vec{S}$ given by LS coupling. The f electrons are completely localized at each ion site. Conduction electrons are assumed to have a simple conduction band with energy $E(\vec{k})$. The interaction between the conduction electrons and the magnetic ions is described by the following Hamiltonian:

$$\mathcal{H} = N^{-1} \sum_n V \delta(\vec{r} - \vec{R}_n)\, \vec{S}_n \cdot \vec{s}_e$$

in which V is an effective exchange energy between a conduction electron of spin $\vec{s}_e$ and the ion at $\vec{R}_n$ and the delta function is an approximation which gives a constant scattering cross section for

all electron collisions. The relaxation time τ is given by the following expression

$$\frac{1}{\tau} = \frac{1}{\tau_i} + \frac{1}{\tau_p} + \frac{1}{\tau_s}$$

where τ_i represents residual impurity scattering (independent of temperature), τ_p represents phonon scattering and is of the form:

$$\frac{1}{\tau_p} \propto T^5 \int_0^{\theta/T} \frac{x^5 dx}{(e^x - 1)(1 - e^{-x})} ,$$

and τ_s represents spin disordering interaction from $\mathcal{H}$, and is approximated by the expression used by Kasuya[40] and de Gennes and Friedel[36]

$$\frac{1}{\tau_s} \propto V^2 \left(1 - \frac{\langle \vec{S} \rangle^2}{(1 + S)S}\right) .$$

Using this model and the type of spin ordering in the rare earth element, an energy band structure is obtained. Then the change in the conductivity tensor

$$\sigma_{ij} = \frac{e^2 \tau}{4 \pi^2 \hbar} \int v_i \, dS_j$$

due to the change in the energy band caused by magnetic ordering is calculated, where the integration is over the Fermi surface, and

$$\vec{v} = \frac{1}{\hbar} \frac{\partial E}{\partial \vec{k}}$$

is the group velocity. The final expression of the resistivity and its temperature dependence is given by three parameters which are to

be determined from the resistivity measurement data. Since the z-axis is along the c-axis of the hcp structure for the rare earth element, the resistivity is given by

$$\rho_{zz} = [\alpha + \beta T + \gamma(1 - \tfrac{1}{2}M^2 - M'^2)][1 - \Gamma(M^2 + M'^2)^{\frac{1}{2}}]^{-1}$$

and

$$\rho_{xx} = \alpha' + \beta' T + \gamma'(1 - \tfrac{1}{2}M^2 - M'^2)$$

with $\Gamma = (3\pi VS/4E_f k_f)\Sigma_i l_i$, where Σ_i sums over all new superlattice boundaries that cut the Fermi surface, and α, β, and γ are constants to be determined from the resistivity data, α from $\rho(T=0)$, β from the slope of the linear part of $\rho(T)$, γ from the $\rho(T=T_N)$, and Γ is assumed to be independent of T. The values of M and M' are taken from the neutron diffraction data, which are concerned with the ordering type of the spin of magnetic ions. The quantitative agreement of this theory with experimental data is not too good, but it gives the proper trend for the resistivity changes over the whole temperature range.

The difference between Elliott's and de Gennes' (or Kasuya's) theories is that Elliott considered the change of the Fermi surface due to the ordering of the spins of the magnetic ions in addition to the spin disordering scattering. The former are able to fit qualitatively the whole range of $\rho(T)$, and the latter are able to predict quantitatively the effect of the spin disordering scattering without considering the whole range of temperature.

In 1963, Smidt and Daane[31] measured the electrical

resistivity of rare earth alloys of Gd-Lu, Tb-Lu, Gd-Er, and Y-Lu systems from 4.2°K to 320°K in order to investigate the effect of the localized magnetic moments in the above systems. And their ρ_s for the systems studied was plotted against the values of an average value of $S^2(J + 1)/J$ for the systems involved. They are not related linearly, and the deviations are similar to the deviations from a linear relation between $S^2(J + 1)/J$ and those ρ_s values of pure rare earth elements.

In 1964, Dekker[43] suggested a model which is based upon the Nordheim approximation[44] (effects due to local atomic or spin order are neglected) to explain the results of Smidt and Daane[31] and of Hennephof[45]. The same form of interaction between conduction electrons and magnetic ions, namely $-2G(|\vec{r} - \vec{R}_n|)\,\vec{s}_e \cdot \vec{S}_n$ as given by Kasuya and de Gennes was used.

In his treatment, Dekker assumed that the conduction electrons behave as electrons of effective mass m^* which are independent of the composition of the alloys, and the atomic volume and number of valence electrons of the components of the alloys are the same. Thus the number of atoms per unit volume N and the electron concentration n, for an alloy of R_xM_{1-x} are independent of x. Finally a disordered solid solution is assumed. The lattice is then divided into R and M cells of equal size. In the cells of R atoms, its potential operator is of the form $V_R(\vec{r}) - 2G\,\vec{s}_e \cdot \vec{S}_n$ and in the cells of M atoms, its potential operator is $V_M(\vec{r})$. The total angular momentum of R atoms are $J = L + S$. At temperatures

higher than the spin ordering temperature, the average potential is assumed of the form of

$$V_p(\vec{r}) = x V_R(\vec{r}) + (1-x)\, V_M(\vec{r}) .$$

Hence, the perturbation due to the spin ordering at temperature lower than the spin ordering temperature is written as

$$\mathcal{H}_R(\vec{r}) = V_R(\vec{r}) - 2G(\vec{r})\,\vec{s}_e\cdot\vec{S}_n - V_p(\vec{r})$$

$$= (1 - x)[\, V_R(\vec{r}) - V_M(\vec{r})\,] - 2G(\vec{r})\,\vec{s}_e\cdot\vec{S}_n ,$$

$$\mathcal{H}_M(\vec{r}) = V_M(\vec{r}) - V_p(\vec{r}) = -x[\, V_R(\vec{r}) - V_M(\vec{r})\,].$$

Then by considering the non-zero matrix elements for the elastic scattering of conduction electrons of the above perturbations, the corresponding differential cross sections $\sigma_i(\varphi)$ are derived, and hence the corresponding relaxation time τ_{if} is obtained:

$$\frac{1}{\tau_{if}} = \frac{\hbar k_f N_i}{m^*} \int_o^{\pi} \sigma_i(\varphi)(1 - \cos\varphi)\, 2\pi \sin\varphi \, d\varphi$$

where the subscript f referred to electrons with Fermi energy. Then the contribution to the resistivity is

$$\rho_i = \frac{m^*}{ne^2\tau_{if}} \quad , \quad i \text{ stands for R or M.}$$

For the spin disordering resistivity at $T \gg T_c$,

$$\rho_s = \frac{m^* k_f N}{\pi \hbar^3 ne^2}\,[\, x(1 - x)|V_{RM}|^2 - x|F|^2(g - 1)^2 j(j + 1)\,]$$

where

$$v_{RM} = \int [\, V_R(\vec{r}) - V_M(\vec{r}) \,] e^{i\,\vec{q}\cdot\vec{r}} d\vec{r}$$

$$F = \int G(\vec{r})\, e^{i\vec{q}\cdot\vec{r}}\, d\vec{r}$$

$$\vec{q} = \vec{k} - \vec{k}' ,$$

with $\vec{k}$, $\vec{k}'$ being the wave vectors of conduction electrons, and j the quantum number for the total angular mementum of the R ion. If we put $x = 1$, this expression will reduce to the similar expression ρ_s of Rocher's, with the interaction constant $|F|^2 = \Gamma^2/4$ and $n = k_f^3/3\pi^2$, $V = N^{-1}$, $E_f = \hbar^2 k_f^2/2m^*$.

At $T = 0$, where the alloys studied by Smidt and Daane and by Hennephof are all ferromagnetic, Dekker suggested the corresponding $V_p(\vec{r})$ as following:

$$V_p(\vec{r}) = x V_R(\vec{r}) + (1 - x)\, V_M(\vec{r}) - 2x G(\vec{r}) m_{es} (g - 1) j$$

since the z-components of the total angular momentum for all R-atoms are equal to j, and the eigen-value of S_z is $(g - 1)j$. This gives the perturbations

$$\mathcal{H}'_{R,\pm}(\vec{r}) = (1 - x)[\, V_R(\vec{r}) - V_M(\vec{r}) \mp G(\vec{r})(g - 1)j \,]$$

$$\mathcal{H}'_{M,\pm}(\vec{r}) = -\, x[\, V_R(\vec{r}) - V_M(\vec{r}) \mp G(\vec{r})(g - 1)j \,]$$

for $m_{es} = +\frac{1}{2}$ or $-\frac{1}{2}$ in the R and M cells respectively. This implies that

$$\frac{1}{T_{f\pm}} = \frac{k_f m^* N\, x(1 - x)}{\pi \hbar^3} \left| v_{RM} \mp F(g - 1)j \right|^2 .$$

For the alloys studied, it is shown that the samples are multi-domained, with small domain size compared to the mean free path of the conduction electrons, and the disordered resistivity due to spatial spin disorder at T= 0 is

$$\rho_s(0) = \frac{m^* k_f N x(1 - x)}{ne^2 \pi \hbar^3} [\,|v_{RM}|^2 - |F|^2 (g - 1)^2 j^2]$$

Comparing the experimental data with the $\rho_s(T \gg T_c)$ and $\rho_s(T= 0)$ it is shown that those resistivity data of Smidt and Daane can be explained by the Nordheim approximation.

The above arguments give a satisfactory explanation for the measured electrical resistivity of the alloys of Gd-Lu, Tb-Lu, and Gd-Y systems of which one of the components of each system is magnetic and the other is not. The explanation is not satisfactory for the Gd-Er alloys, because both the components are magnetic. Dekker has treated the case of 2 magnetic components, and obtained a satisfactory explanation. However, as in the treatment of Rocher [35], only the contribution of the spin disordering effect on the resistivity was considered and the complete relationship between resistivity and temperature has not been studied.

VI. ANALYSIS OF THE ANTIFERROMAGNETIC TRANSITION IN CSCL PHASES CONTAINING RARE EARTH ELEMENTS

The CsCl type crystal structure can be considered as an ordered body centered cubic structure. In this structure the different kinds of ions are separated by a distance of $\frac{1}{2}\sqrt{3}a$ and the same kind of ions are at a distance a (the lattice parameter) from each other. As it was explained in Section II, the metal ions (expressed by M) other than rare earth elements (expressed by R) enter into this structure with a characteristic value r_M, independent of the particular rare earth element. In the case of Cu, Ag and Au, the analyses given there show that $(r_M)_{Cu} = 2.09\,A$, $(r_M)_{Ag} = 2.215\,A$ and $(r_M)_{Au} = 2.172\,A$, where r_M was expressed as the difference between the nearest neighbour distances (namely $\frac{1}{2}\sqrt{3}a$) and the trivalent ionic radii (r_E) of rare earth elements, and is a constant for a given M element. From the neutron diffraction analysis of these compounds (see TABLE 11) we know that the R-ions are almost trivalent, hence the use of the trivalent ionic radii of rare earth elements is allowable. And the M-ions are possibly deformed by the presence of the rare earth ions due to the indirect exchange interaction through the conduction electrons.

Since the electrical resistivity of these alloys is relatively low it is reasonable to assume that the bonding is predominant, and hence the M-ions may be assumed to be monovalent as usual. On the other hand, the rare earth ions are magnetic due to the deeply buried unfilled 4f electron shells, the $4f^n$ electrons are

TABLE 11

Comparison of the Magnetic Moment of Rare Earth Ions in CsCl Phases and in Pure Elements

Phases	μ'	μ	$(\mu'/\mu)\%$
CuTb	9.0	9.7	93
CuDy	8.0	10.64	76
CuEr	8.5	9.5	89
AgTb	9.0	9.7	93
AgDy	9.7	10.64	92
AgEr	7.4	9.5	77

μ' is the magnetic moment (in Bohr magneton) of the rare earth ion in CsCl phases. Data from neutron diffraction analysis by J. W. Cable, private communication.

μ is the experimental value of the magnetic moment (in Bohr magneton) of the trivalent rare earth ion in pure elements. Data from page 45 of reference (3).

localized on each ion site in the lattice. The M-ions have filled d shells. We may assume that each pair of R and M ions contributes 4 conduction electrons, 3 from R-ion and one from M-ion. The magnetic property of some of these compounds has been studied by neutron diffraction[23],[33] and it is known that all the investigated phases are antiferromagnetic of $(\pi, \pi, 0)$ type as $T \leq T_N$.

According to the above statements and the fact that the resistivity-temperature curves show definite anomalies (see Section III) the indirect exchange mechanism similar to that of the pure rare earth element and alloys may be put in order. Let $\vec{J}_n$ be the total angular momentum of the n-th rare earth ions at $\vec{R}_n$ with J_n as its quantum number, $\vec{I}_m$ the nuclear spin of the M-ions at $\vec{R}_m$ with quantum number $\vec{I}_m$, and $\vec{s}_e(\vec{r})$ the spin of the conduction electrons at $\vec{r}$. Then the conduction electrons will interact with the unfilled 4f electrons of R-ions at $\vec{R}_n$ with the de Gennes' and Kasuya type interaction $-(g-1)\Gamma\vec{J}_n \cdot \vec{s}_e$ and also interact with the nuclear spins of M-ions at site $\vec{R}_m$ with the similar interaction[39] of $\Gamma'\vec{I}_m \cdot \vec{s}_e$. Then the unfilled 4f electrons and the M-ions will feel the existence of the other localized 4f shells and of the nuclear spins of M-ions due to the polarization of the conduction electrons. The corresponding indirect exchange interactions following the suggestion of Yosida will be of the form of $A\vec{J}_n \cdot \vec{J}_{n'} F(2k_m R_{nn'})$, $B\vec{J}_n \cdot \vec{I}_m F(2k_m R_{nm})$ and $C\vec{I}_m \cdot \vec{I}_{m'} F(2k_m R_{mm'})$, where A, B, C are constants involving the Fermi energy and the exchange integrals, $F(\xi)$ are the Ruderman-Kittel function, and k_m is the maximum wave vector of the conduction electrons. The antiferromagnetic ordering can be taken into consid-

eration either by spin-wave methods or by the use of the Ising model, and this ordering has to be considered before we can have a meaningful comparison between the theory and the experimental results, the ρ_s and the transition temperatures, and possibly the whole course of the resistivity temperature relationship.

However, if the path of Elliott and Wedgwood[42] is to be considered, we may have the following model to explore the experimental results, although no detail can be carried out because of lack of complete information about the relaxation time of the conduction electrons. As mentioned above, the 4f electrons are assumed to be localized at each rare earth ion site which is described by the total angular momentum $\vec{J}_n$, and the M-ions are specified by their nuclear spin $\vec{I}_m$. The conduction electrons are then assumed to be described by the use of a conduction band of energy $E(\vec{k})$. The detailed expression of $E(\vec{k})$ or the shape of Fermi surface can not be given at this stage.

The interaction between the conduction electrons and the ions will be given by

$$\mathcal{H} = \frac{1}{N}\sum_n V\delta(\vec{r}-\vec{R}_n)\vec{J}_n \cdot \vec{s}_e - \frac{1}{N}\sum_m V'\delta(\vec{r}-\vec{R}_m)\vec{I}_m \cdot \vec{s}_e$$

where V, V' are the effective exchange energy between a conduction electron of spin $\vec{s}_e$ and the rare earth ions of total angular momentum $\vec{J}_n$, and nuclear spin $\vec{I}_m$ of M-ions respectively. N is the number of the R-ions or M-ions per unit volume and delta function is an approximation that will give a constant scattering cross section for all electron collisions. The relaxation time τ will be considered as following

$$\frac{1}{\tau} = \frac{1}{\tau_i} + \frac{1}{\tau_p} + \frac{1}{\tau_s}$$

with τ_i due to impurities and lattice imperfections which is independent of T, and τ_p due to the electron-phonon interaction, expressed by the Grüneisen function. τ_s is the part due to the spin disorderings according to the given interactions given above. Its explicit expression can not be given at this moment. From experimental facts, most of the CsCl phases as given in TABLE 9 are antiferromagnetic at $T < T_N$ with the rare earth ions in neighboring ferromagnetic planes $\{ 110 \}$ in opposite direction (parallel or anti-parallel to the $[001]$ direction). For a better explanation of the experimental results on $\rho(T)$, this ordering has to be taken into consideration through τ_s.

In the following TABLE (TABLE 12) the experimental data of ρ_s of pure rare earth elements and of the corresponding RM alloys along with other figures are given. As shown in Figure 27, the ρ_s vs. $(g-1)^2 J(J+1)$ plot has large deviations from linearity. We investigated this fact by the use of the de Gennes' model. The expression

$$\rho_s = \frac{3\pi}{8} \frac{m^*}{\hbar e^2} \Gamma^2 \frac{(g-1)^2}{V E_f} J(J+1)$$

which was applied to pure rare earth elements by Rocher[35] with success, apparently is not satisfactory when applied to the present results. That means if we do use the same type of interaction mechanism, the m* and Γ are essentially not constant for each series of RM for a given M. From the differences between the

TABLE 12

Resistivity of CsCl Phases and of Pure Rare Earth Elements Due to Spin-Disorder Scattering

	ρ_s ($\mu\Omega$ - cm)				$(g-1)^2J(J+1)$	J	S	g	$(\rho_s)_{R.E.}/(\rho_s)_{RM}$		
	Pure R. E.	CuR	AgR	AuR					CuR	AgR	AuR
Gd	106.4	28.7	14.2	21.5	15.75	7/2	7/2	2	4	8	5
Tb	85.7	9.9	13.3	16.7	10.5	6	3	3/2	9	7	5
Dy	57.6	4.4	4.6	2.4	7.08	15/2	5/2	4/3	13	13	24
Ho	32.3	0.6	0.4	0.6	4.5	8	2	5/4	54	80	54
Er	23.6	---	-0.4	-1.6	2.55	15/2	3/2	6/5	--	-61	-15
Tm	14.9	-1.0	-1.4	-0.8	1.67	6	1	7/6	-15	-10	-18

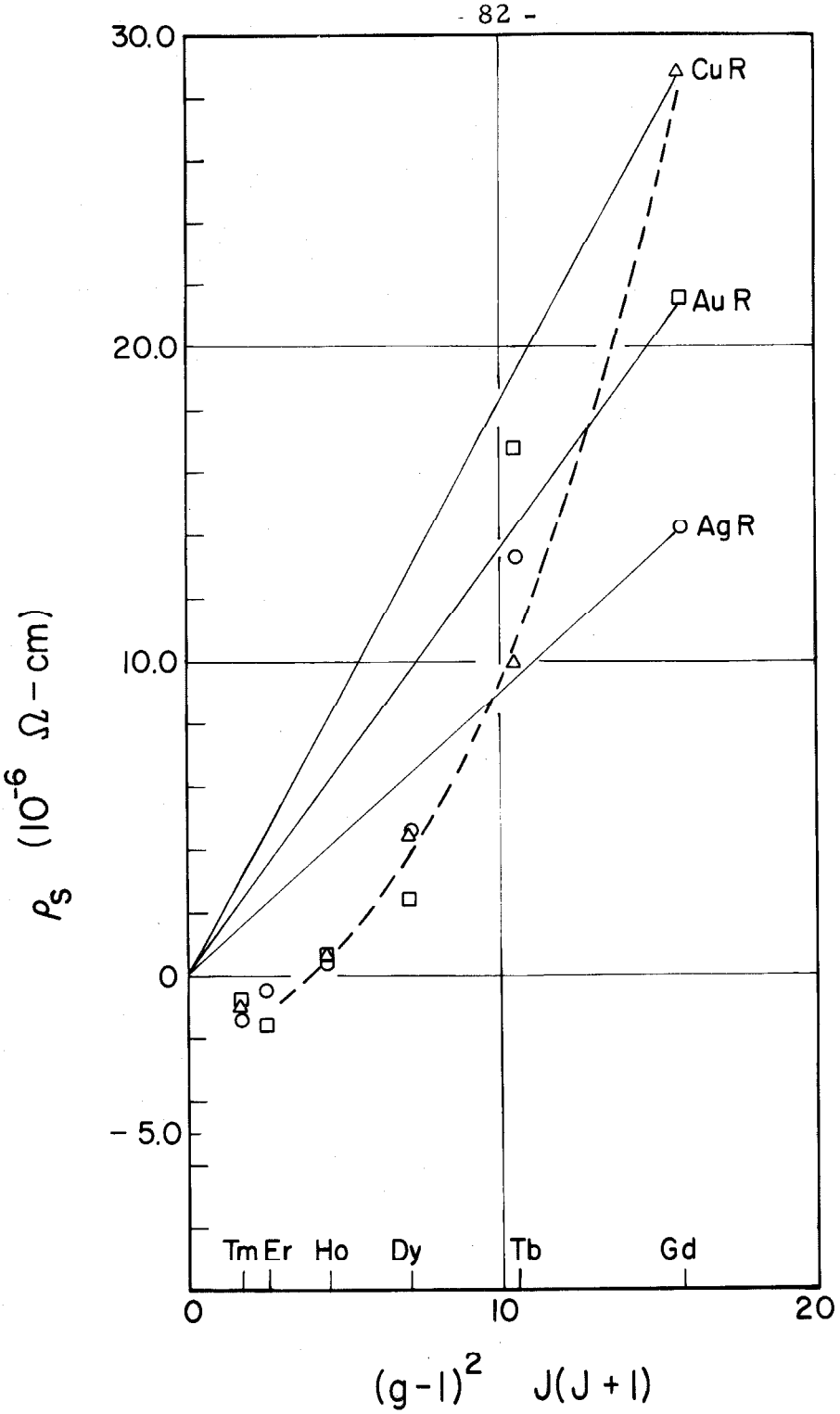

Fig. 27. The Relationship Between The Resistivity due to The Spin-Disorder Scattering and The Value of $(g-1)^2J(J+1)$ of Rare Earth Ions in CsCl Phases

ρ_s of GdM and TbM for M = Cu, Ag, Au, it is obvious that the influence of M-ions in the lattice cannot be considered all alike. On the other hand the influence of M-ions in Dy, Ho, Er, Tm is nearly the same for M = Cu, Ag, Au.

From Figure 27, it is seen that for CuR, the ρ_s vs. $(g-1)^2J(J+1)$ plot seems to follow a smooth curve which is parabolic; but for AuR and AgR the similar trend exists only up to R = Tb, and Gd is excluded. Since GdAg is known as antiferromagnetic from the magnetic susceptibility measurement by Walline, we may assume that the S-like relation between ρ_s and $(g-1)^2J(J+1)$ of RAg and RAu phases is normal for antiferromagnetism and CuGd is quite possibly not antiferromagnetic for temperature lower than the transition temperature. Magnetic susceptibility measurements will make this point clear. Expecting a linear relationship between ρ_s of RM phases and $(g-1)^2J(J+1)$ is equivalent to the assumption that we are neglecting the existence of M-ions in the lattice and all its effects, and also that we are treating the remaining rare earth ions as in a simple cubic arrangement with the given lattice parameter a.

Another interesting point is that the ρ_s values for RM compounds are very small comparing with the ρ_s values for the corresponding rare earth elements. This would be due to the influence of the M-ions. The Fermi surface (which directly influences τ_s) must deviate considerably from the assumed spherical shape.

VII. CONCLUSIONS

In this study, thirty-nine new phases crystallizing in the CsCl type structure and containing one rare earth metal have been found. In agreement with previously published results on a limited number of CsCl phases containing rare earth metals, the lattice parameters of the new phases increased linearly with the trivalent ionic radii of the rare earth metals. No theoretical explanation for this linear relationship has been found so far, but it is suggested that the metallic ions in the structure (other than the rare earth one) are polarized and deformed by the presence of the rare earth ions through an indirect exchange interaction of the conduction electrons.

In the second part of this investigation, electrical resistivity of nineteen CsCl phases of rare earth elements with copper, silver and gold were measured between 4.2°K and about 250°K. With the exception of the phase yttrium-silver, all the CsCl phases studied showed an anomaly in the resistivity-temperature curve. At temperatures below this anomaly, the CsCl phases are most probably antiferromagnetic. The anomaly in resistivity is due to the change in the scattering of the conduction electrons resulting from the disordering of the spins of the magnetic ions (rare earth ions) above the transition temperature. The postulated existence of an antiferromagnetic transition in CsCl phases involving rare earth ions is discussed on the basis of published studies of neutron diffraction, as well as magnetic susceptibility measurements, of some of these phases. Qualitative explanations for the electrical

resistivity anomalies were attempted, based on the indirect exchange interaction between the ions of the same type and between the ions of different type (magnetic and non-magnetic). Possible modifications to the theory were suggested in order to improve the agreement between theory and experimental results. The most fruitful experimental studies to carry out on the CsCl phases appear to be measurements of magnetic susceptibility, magnetoresistivity and specific heat of these alloys across the transition temperatures.

REFERENCES

1. C. C. Chao, H. L. Luo, P. Duwez, J. Appl. Phys. (1963) 34, 1971.

2. C. C. Chao, H. L. Luo, P. Duwez, J. Appl. Phys. (1964) 35, 257.

3. K. A. Gschneidner Jr., Rare Earth Alloys (D. Van Nostrand Company, Inc. Princeton, New Jersey, 1961)

4. A. Iandelli, in Rare Earth Research, edited by E. V. Kleber (The Macmillan Company, New York, 1961) p. 135.

5. H. Nowotny, Z. Metallk. (1942) 34, 247.

6. A. Rossi, Gazz. chim. ital. (1934) 64, 774.

7. F. Mahn, Ann. Phys. (1948) 3, 396.

8. A. Iandelli, Paper No. 3F, pp. 3F in The Physical Chemistry of Metallic Solution and Intermediate Compounds, (Her Majesty's Stationary Office, London, 1959)

9. E. D. Gibson, O. N. Carlson, Trans. ASM (1960) 52, 1084.

10. A. E. Miller, A. H. Daane, Trans. AIME (1964) 230, 568.

11. F. Gaume-Mahe, M. Cohen, J. recheres centre nat. recherche sci. (Labs. Bellevue, Paris, 1957) No. 38, 64.

12. J. H. N. Van Vucht, Z. Metallk (1957) 48, 253.

13. P. W. Stillwell, E. E. Jukkola, J. Am. Chem. Soc. (1934) 56, 56.

14. R. D. Grinthal, WADC-TR-53-190 (American Electro Metal Division, Firth Sterling, Inc. Report) Part VI (May, 1958)

15. R. F. Domagala, J. J. Rausch, D. W. Levinsov, Trans. ASM (1961) 53, 137.

16. A. Indelli, E. Botti, Gazz chim. ital. (1937) 67, 638.

17. A. E. Dwight, Trans. AIME (1959) 215, 283.

18. A. Iandelli, Atti congr. intern. chim., 10th Congr. Rome (1938) 2, 688.

19. H. Bommer, E. Krose, Z. anorg. Chem. (1943) 252, 62.

20. R. Ferro, Gazz. chim. ital. (1955) 85, 888.

21. N. C. Baenziger, J. L. Moriarty, Jr., Acta Cryst (1961) 14, 948.

22. A. Iandelli, R. Ferro, Atti accad. nazl. Lincei Rend. (Classe sci. fis. mat. e nat., 1951) 10, 48.

23. J. W. Cable, W. C. Kochler, E. O. Wollan, Phys. Rev. (1964) 136, A240.

24. V. B. Compton, Acta Cryst (1958) 11, 446.

25. M. V. Nevitt, in Electronic Structure and Alloy Chemistry of The Transition Elements, edited by Paul A. Beck (John Wiley & Sons, New York, London, 1963) p. 140.

26. R. V. Colvin, Sigurds Arajs, J. Appl. Phys., (1963) 34, 286.

27. F. H. Spedding, S. Legvold, A. H. Danne, L. D. Jennings in Progress in Low Temperature Physics, Vol. II, edited by C. J. Gorter (North-Holland Publishing Co., 1957) p. 368.

28. M. A. Curry, S. Legvold, F. H. Spedding, Phys. Rev. (1960) 117, 953.

29. R. V. Colvin, S. Legvold, F. H. Spedding, Phys. Rev. (1960) 120, 741.

30. J. K. Alstad, R. V. Colvin, S. Legvold, F. H. Spedding, Phys. Rev. (1961) 121, 1637.

31. F. A. Smidt, Jr., A. H. Danne, J. Phys. Chem. Solids (1963) 24, 361.

32. R. L. Powell, M. D. Bunch, R. J. Corruccini, Cryogenics (March, 1961) p. 139.

33. J. W. Cable (Oak Ridge National Laboratory), private communication, September 23, 1964.

34. R. E. Walline (University of Pittsburgh), private communication, July, 1964.

35. Yves-Andre Rocher, Advances in Physics (1962) 11, 233.

36. P. G. De Gennes, J. Friedel, J. Phys. Chem. Solids (1958) 4, 71.

37. P. G. De Gennes, Comptes Rendus Acad. Sci. (Paris, 1958) 247, 1836.

38. C. Kittel, Quantum Theory of Solids (John Wiley & Sons, Inc., New York, 1963) p. 360.

39. K. Yoshida, Phys. Rev. (1957) 106, 893.

40. T. Kasuya, Progress Theoretical Physics (1956) 16, 45; 58.

41. T. Kasuya, Progress Theoretical Physics (1956) 16, 58.

42. R. J. Elliott, F. A. Wedgewood, Proc. Phys. Soc. (1963) 81, 846.

43. A. J. Dekker, phys. stat. sol. (1964) 7, 241.

44. L. Nordheim, Ann. Phys. (1931) 9, 607.

45. J. Hennephof, Phys. Letters (Netherlands, 1964) 11, 273.